PERGAMON

International Journal of Solids and Structures 38 (2001) 717–739

INTERNATIONAL JOURNAL OF SOLIDS and STRUCTURES

www.elsevier.com/locate/ijsolstr

A mixed variational method for linear coupled thermoelastic analysis

Agostino Antonio Cannarozzi, Francesco Ubertini *

Facoltà di Ingegneria, Università degli Studi di Bologna, DISTART-Scienza delle Costruzioni, Viale Risorgimento 2, 40136 Bologna, Italy

Received 6 October 1999; in revised form 22 February 2000

Abstract

A variational method for linear coupled quasi-static thermoelastic analysis is presented. The variational support is a statement in terms of displacement, temperature, stress and heat flux. The statement is based on the hybrid stress formulation for the elastic part and on the mixed flux–temperature formulation for the thermal one, and includes the rate dependent terms of the energy balance equations and the initial condition. A finite element model for the semi-discrete analysis is developed within this variational framework, and a guideline for implementing a family of thermoelastic finite elements is given. Some test cases enlighten the effectiveness and reliability of the approach proposed. © 2000 Elsevier Science Ltd. All rights reserved.

Keywords: Thermoelasticity; Variational method; Mixed model; Finite element

1. Introduction

Thermal stresses play a specific role in solid mechanics (Boley and Weiner, 1960; Nowacki, 1986). In the case of traditional materials, thermal effects on a body are limited to strains due to the temperature gradient, which is autonomously determined and constitutes a datum for stress analysis. In the case of sophisticated materials (e.g. high performance composites), thermal effects can include heat production due to strain rate, i.e. the thermoelastic dissipation. In this case, thermal and stress analyses are coupled. An analytical treatment of such problems is hardly ever possible for reasons of mathematical complexity, so that the development of alternative methods of analysis is essential. On this purpose, a variational formulation of the coupled thermoelastic problem can be of interest, both as a theoretical contribution and as a sound support for a suitable method of analysis.

With regard to the first aspect, Biot (1956) first gave a variational principle for the coupled problem of thermoelasticity, in terms of displacement and entropy flow. Further, contributions of Herrmann (1963) and Ben-Amoz (1965) generalize Biot's principle. Principles à la Gurtin were given by Iesan (1966), Nickell and Sackman (1968), Rafalski (1968) – see also the survey paper of Carlson (1972). By introducing the heat

* Corresponding author. Fax: +390-51-644-3495.
E-mail address: francesco.ubertini@mail.ing.unibo.it (F. Ubertini).

0020-7683/01/$ - see front matter © 2000 Elsevier Science Ltd. All rights reserved.
PII: S0020-7683(00)00061-5

displacement (a vector function whose divergence is, by definition, the temperature) as a variable, Keramidas and Ting (1976) presented a variational principle in displacements and in this new variable, and derived a finite element model. From a different side, Askar Atlay and Cengiz Dökmeci (1996) have provided for a comprehensive framework of variational principles in the standard kinematic, dynamic and thermal variables.

The variational approach chiefly followed in the applications seems to be the compatible one, i.e. in displacement and temperature (e.g. Carter and Booker, 1989; Tamma and Namburu, 1991; Tay, 1992; Rao and Sinha, 1997), certainly for its simplicity and versatility. The possibility of combining the assumed strain mixed approach (Atluri et al., 1983) with the customary temperature approach (Hogge and Fraeijs de Veubeke, 1972) is presented by Zhu and Cescotto (1995), with emphasis on the finite element implementation for stress analysis and only a marginal consideration for thermoelastic coupling. More recently, the authors have presented a mixed finite element model for thermoelastic analysis (Cannarozzi and Ubertini, 1998), which anticipates some issues exposed in the sequel.

This paper moves from the authors' opinion that a procedure of analysis which involves directly both primal variables – displacement and temperature in this case – and dual variables – stress and heat flux – can be more convenient, not only for obtaining a better accuracy in the results, but also for the possibility of controlling independently all the quantities involved in a process. On this premise, the paper presents an integrated, mixed method for treating linear coupled thermoelastic problems in the quasi-static case – the inertia terms are disregarded. Indeed, this case can be meaningful for real materials (Atarashi and Minagawa, 1992), and especially for non-traditional ones. The method is essentially based on the Hellinger–Reissner principle in the hybrid version (Atluri et al., 1983) – modified minimum complementary energy principle – for the elastic part, and on the analogous principle in heat conduction (Fraeijs de Veubeke and Hogge, 1972) for the thermal one. So, the field variables of the variational problem, on the whole, are stress, heat flux and temperature, and the boundary variables are displacement and temperature. The variational statement which supports the method encompasses: the functionals of the above principles, a functional which takes into account the thermoelastic dissipation and the energy related to the temperature rate, and a functional accounting for the initial temperature condition. Stresses are assumed in equilibrium with the field load, according to the hybrid stress model. As is well known, one of the advantages of this approach is to be free of locking. The thermoelastic dissipation is expressed in terms of stress rate via constitutive law to eliminate strain rate as a field variable. For the rate dependent terms, the energy balance is enforced weakly by employing the temperature as a Lagrange multiplier, whereas thermal equilibrium for field heat sources is fulfilled in advance, so that the approach on the thermal side is of mixed type, and becomes formally of hybrid type for the steady state problem. This last approach has been experienced with satisfactory results and proposed by the authors (Cannarozzi et al., 1999, 2000) in heat conduction analysis. In the finite element discretization, temperature within the element and temperature at the interelement are represented independently of each other. This aims at improving the thermal response of the model without affecting the consistency between stress and temperature representations (de Miranda and Ubertini, 1999). Stress and heat flux parameters are eliminated at the element level. Thus, at the assembly level, the statement yields, besides the initial conditions, the discretized energy balance equations and the interelement equilibrium equations for stresses and heat flux and involves the inner temperature and the interelemental displacement and temperature. The integration in the time domain can be implemented following a method with variational support (e.g. Ubertini, 1998; Mancuso et al., 1998), as well as a finite difference based procedure (e.g. Hughes, 1987).

Entering into the details of the exposition, Section 2 accounts for the equations of the initial–boundary value problem. The corresponding variational formulation is given in Section 3, and the relevant mixed model is exposed in Section 4. A finite element implementation is developed and discussed with regard to stability, consistency and invariance in Section 5. Some numerical tests, exposed in Section 6, account for the superior convergence and accuracy properties of the proposed finite element scheme in comparison with

the compatible model, with particular regard to mesh distortion sensitivity. This shows that the higher computational expense is widely offset by the quality in the results. Some concluding remarks end the paper.

2. The initial–boundary value problem

Consider a body which at the time $t = 0$ occupies the closed and bounded domain $\bar{B}$ of the euclidean space $\mathbb{R}^n$ ($n = 1, 2, 3$). The inner part of $\bar{B}$ is denoted by B and its boundary by ∂B, $B \cup \partial B = \bar{B}$. The measure of B is V and the measure of ∂B is S. The space is referred to a cartesian coordinate system $(O; x_i, i = 1, \ldots, n)$, and a point of $\bar{B}$ is indicated by the vector $\mathbf{x}$ of its coordinates. The time interval of interest is $\bar{I} = [0, t_f)$, and its open set is denoted by $I = (0, t_f)$.

The state of the body is described by the displacement vector $\mathbf{u}(\mathbf{x}, t)$ and the temperature $T(\mathbf{x}, t)$, in $\bar{B} \times \bar{I}$, and by the strain tensor $\boldsymbol{\epsilon}(\mathbf{x}, t)$, the stress tensor $\boldsymbol{\sigma}(\mathbf{x}, t)$ and the heat flux vector $\mathbf{q}(\mathbf{x}, t)$, in $B \times \bar{I}$. Tensors $\boldsymbol{\epsilon}$ and $\boldsymbol{\sigma}$ are symmetric. Contact force and thermal flux through an interface are $\boldsymbol{\sigma}\mathbf{n}$ and $\mathbf{q} \cdot \mathbf{n}$, respectively, where $\mathbf{n}$ is the unit outward normal vector on the interface.

The distributed load $\mathbf{p}(\mathbf{x})$, independent of t, and the heat source $\gamma(\mathbf{x}, t)$ are prescribed in B. The boundary ∂B is subdivided into five parts, independent of t: ∂B_u, ∂B_t, and ∂B_T, ∂B_q, ∂B_c, such that $\partial B_u \cup \partial B_t = \partial B_T \cup \partial B_q \cup \partial B_c = \partial B$, $\partial B_u \cap \partial B_t = \emptyset$, and the mutual intersections among ∂B_T, ∂B_q and ∂B_c are empty. The displacement $\bar{\mathbf{u}}(\mathbf{x})$ and the traction $\bar{\mathbf{t}}(\mathbf{x})$, both independent of t, are prescribed on ∂B_u and ∂B_t, respectively. The temperature $\bar{T}(\mathbf{x}, t)$, the contact flux $\bar{q}(\mathbf{x}, t)$, and the convective flux $\kappa(T - T_c)$, where $\kappa(> 0)$ is the convective exchange coefficient and T_c is the temperature of the surrounding medium, are prescribed on ∂B_T, ∂B_q and ∂B_c, respectively. Temperature T_c is independent of $\mathbf{x}$ and t.

The transient thermoelastic problem (Carlson, 1972) consists in determining the response of the body in terms of $\mathbf{u}$, T, $\boldsymbol{\epsilon}$, $\boldsymbol{\sigma}$, $\mathbf{q}$ due to the above data, according to the following relationships in I:

compatibility equations

$$\boldsymbol{\epsilon} = \operatorname{symgrad} \mathbf{u} \quad \text{in } B, \tag{1}$$

$$\mathbf{g} = \operatorname{grad} T \quad \text{in } B, \tag{2}$$

$$\mathbf{u} = \bar{\mathbf{u}} \quad \text{on } \partial B_u, \tag{3}$$

$$T = \bar{T} \quad \text{on } \partial B_T, \tag{4}$$

where $\mathbf{g}$ is the heat strain vector (the analogue of strain $\boldsymbol{\epsilon}$),

equilibrium and thermal balance equations

$$\operatorname{div} \boldsymbol{\sigma} + \mathbf{p} = \mathbf{0} \quad \text{in } B, \tag{5}$$

$$-\operatorname{div} \mathbf{q} + \gamma - T_0 \mathbf{C}\mathbf{A} \cdot \dot{\boldsymbol{\epsilon}} - \rho c \dot{T} = 0 \quad \text{in } B, \tag{6}$$

$$\boldsymbol{\sigma}\mathbf{n} = \bar{\mathbf{t}} \quad \text{on } \partial B_t, \tag{7}$$

$$\mathbf{q} \cdot \mathbf{n} = \bar{q} \quad \text{on } \partial B_q, \tag{8}$$

$$\mathbf{q} \cdot \mathbf{n} = \kappa(T - T_c) \quad \text{on } \partial B_c, \tag{9}$$

constitutive equations

$$\boldsymbol{\sigma} = \mathbf{C}[\boldsymbol{\epsilon} - \mathbf{A}(T - T_0)], \tag{10}$$

$$\mathbf{q} = -\mathbf{k}\mathbf{g}, \tag{11}$$

with the initial temperature condition, at $t = 0$,

$$T|_0 = \bar{T}_0 \quad \text{in } B, \tag{12}$$

where $\mathbf{C}$ is the tensor of the elastic stiffness moduli, $\mathbf{k}$, the tensor of the conductivity moduli, $\mathbf{A}$, the tensor of the thermal expansion coefficients, c, the specific heat, ρ, the material density, T_0, the constant reference temperature at which the body is assumed to be free of stresses, $\bar{T}_0$, the initial temperature, $\mathbf{n}$, the unit outward normal vector on ∂B, and the superimposed dot means differentiation with respect to time. Tensor $\mathbf{C}$ is symmetric and positive definite, and the same features are assumed for tensor $\mathbf{k}$ (Prigogine, 1961). Moreover, tensor $\mathbf{A}$ is symmetric, specific heat c and material density ρ are positive.

The differential operators in Eqs. (1), (2), (5) and (6) are connected by the bilinear (Gauss–Green) identities:

$$\int_B \mathbf{v}\cdot\operatorname{div}\mathbf{W}\,\mathrm{d}V = -\int_B \operatorname{symgrad}\mathbf{v}\cdot\mathbf{W}\,\mathrm{d}V + \int_{\partial B}\mathbf{v}\cdot\mathbf{W}\mathbf{n}\,\mathrm{d}S, \tag{13}$$

$$\int_B v\operatorname{div}\mathbf{w}\,\mathrm{d}V = -\int_B \operatorname{grad}v\cdot\mathbf{w}\,\mathrm{d}V + \int_{\partial B} v\mathbf{w}\cdot\mathbf{n}\,\mathrm{d}S, \tag{14}$$

where v, $\mathbf{v}$ and $\mathbf{w}$, $\mathbf{W}$ are respectively a function, two vectors of functions and a symmetric tensor of functions of $\mathbf{x}$, which are assumed to be sufficiently regular.

All the material moduli and quantities in the previous equations are assumed to be constant with respect to $\boldsymbol{\epsilon}$ and T. Under this assumption, the problem described by Eqs. (1)–(12) is linear.

If $\mathbf{g}$ is eliminated between Eqs. (2) and (11), Fourier's law is obtained. By eliminating strain $\boldsymbol{\epsilon}$ between Eqs. (10) and (6), the thermal balance equation can be rewritten as

$$-\operatorname{div}\mathbf{q} + \gamma - T_0\mathbf{A}\cdot\dot{\boldsymbol{\sigma}} - \chi\rho c\dot{T} = 0, \tag{15}$$

where the coefficient $\chi = 1 + T_0(\rho c)^{-1}\mathbf{C}\mathbf{A}\cdot\mathbf{A}$ is greater than one.

In the energy balance Eq. (6), the third term accounts for the mechanical energy involved in the thermoelastic coupling – thermoelastic coupling term. The consequence of the coupling is that thermal and stress analyses should be simultaneously carried out. Dropping the thermoelastic coupling term leads to the semicoupled theory, suitable for conventional materials, where the temperature is separately determined through thermal analysis alone and subsequently prescribed for stress analysis.

3. The variational formulation

The formulation developed in this section is specifically aimed at mixed finite element models in the space domain.

The linear coupled thermoelastic problem can be rephrased in terms of displacement $\mathbf{u}$, temperature T, stress $\boldsymbol{\sigma}$ and heat flux $\mathbf{q}$ by means of the variational (Petrov–Galerkin) statement:

$$\int_I \delta\left[\Pi^E(\mathbf{u},\boldsymbol{\sigma}) + \Pi^T(T,\mathbf{q})\right]\mathrm{d}t + \int_I G\,\mathrm{d}t - C_0 = 0 \quad \forall(\delta\mathbf{u},\delta\boldsymbol{\sigma},\delta T,\delta\mathbf{q}), \tag{16}$$

where

$$\Pi^E(\mathbf{u},\boldsymbol{\sigma}) = -\frac{1}{2}\int_B \boldsymbol{\sigma}\cdot\mathbf{C}^{-1}\boldsymbol{\sigma}\,\mathrm{d}V - \int_B \boldsymbol{\sigma}\cdot\mathbf{A}(T-T_0)\,\mathrm{d}V - \int_B \mathbf{u}\cdot(\operatorname{div}\boldsymbol{\sigma}+\mathbf{p})\,\mathrm{d}V + \int_{\partial B_u}\boldsymbol{\sigma}\mathbf{n}\cdot\bar{\mathbf{u}}\,\mathrm{d}S + \int_{\partial B_t}(\boldsymbol{\sigma}\mathbf{n}-\bar{\mathbf{t}})\cdot\mathbf{u}\,\mathrm{d}S \tag{17}$$

is the Hellinger–Reissner functional (Washizu, 1982),

$$\Pi^T(T,\mathbf{q}) = -\frac{1}{2}\int_B \mathbf{q}\cdot\mathbf{k}^{-1}\mathbf{q}\,\mathrm{d}V + \int_B T(\mathrm{div}\,\mathbf{q}-\gamma)\,\mathrm{d}V - \int_{\partial B_T}\bar{T}\mathbf{q}\cdot\mathbf{n}\,\mathrm{d}S - \int_{\partial B_q} T(\mathbf{q}\cdot\mathbf{n}-\bar{q})\,\mathrm{d}S - \int_{\partial B_c}\left[T\mathbf{q}\cdot\mathbf{n} - \frac{1}{2}\kappa(T-T_c)^2\right]\mathrm{d}S \tag{18}$$

is the analogous, mixed functional in heat conduction (Fraeijs de Veubeke and Hogge, 1972), the functional

$$G(\mathbf{u},T,\delta T) = \int_B \left[T_0\mathbf{C}\mathbf{A}\cdot(\mathrm{symgrad}\ \mathbf{u})^{\cdot} + \rho c\dot{T}\right]\delta T\,\mathrm{d}V \tag{19}$$

takes into account the thermoelastic coupling and the rate of thermal energy, and the functional

$$C_0(T,\delta T) = \int_B \rho c(T|_0 - \bar{T}_0)\,\delta T|_0\,\mathrm{d}V \tag{20}$$

introduces the initial temperature datum. Notice that the functional Π^E should not be varied with respect to T, as the term $\mathbf{A}(T-T_0)$ does play the role of initial strain for the elastic problem. By assuming functions $\mathbf{u}$, $\boldsymbol{\sigma}$, T and $\mathbf{q}$ sufficiently regular in B for identities (13) and (14), the variation of functionals (17) and (18) yields for statement (16) the explicit form:

$$\begin{aligned}\int_I \Bigg\{ &\int_B \delta\boldsymbol{\sigma}\cdot[-\mathbf{C}^{-1}\boldsymbol{\sigma} + \mathrm{symgrad}\,\mathbf{u} - \mathbf{A}(T-T_0)]\,\mathrm{d}V - \int_{\partial B_u}\delta\boldsymbol{\sigma}\mathbf{n}\cdot(\mathbf{u}-\bar{\mathbf{u}})\,\mathrm{d}S + \int_B \delta\mathbf{u}\cdot(\mathrm{div}\,\boldsymbol{\sigma}+\mathbf{p})\,\mathrm{d}V \\ &+ \int_{\partial B_t}\delta\mathbf{u}\cdot(\boldsymbol{\sigma}\mathbf{n}-\bar{\mathbf{t}})\,\mathrm{d}S - \int_B \delta\mathbf{q}\cdot\left(\mathbf{k}^{-1}\mathbf{q} + \mathrm{grad}\,T\right)\mathrm{d}V + \int_{\partial B_T}\delta\mathbf{q}\cdot\mathbf{n}(T-\bar{T})\,\mathrm{d}S \\ &+ \int_B \delta T[\mathrm{div}\,\mathbf{q} - \gamma + T_0\mathbf{C}\mathbf{A}\cdot(\mathrm{symgrad}\,\mathbf{u})^{\cdot} + \rho c\dot{T}]\,\mathrm{d}V - \int_{\partial B_q}\delta T(\mathbf{q}\cdot\mathbf{n}-\bar{q})\,\mathrm{d}S \\ &- \int_{\partial B_c}\delta T[\mathbf{q}\cdot\mathbf{n} - \kappa(T-T_c)]\,\mathrm{d}S\Bigg\}\,\mathrm{d}t - \int_B \delta T|_0\rho c(T|_0-\bar{T}_0)\,\mathrm{d}V = 0 \quad \forall(\delta\mathbf{u},\delta\boldsymbol{\sigma},\delta T,\delta\mathbf{q}),\end{aligned} \tag{21}$$

which results in Eqs. (1)–(12). As a consequence, the solution of problem (1)–(12) meets statement (16) – necessary and sufficient condition.

The requirements of regularity in space for functions $\mathbf{u}$, T, $\boldsymbol{\sigma}$, $\mathbf{q}$, and their variations in Eq. (16), can be relaxed on a finite number of interfaces in B, for semidiscretization through finite elements. On this regard, domain B is subdivided into E non-overlapping open subdomains B_e, $e=1,\ldots,E$, with boundary ∂B_e, $\bar{B}_e = B_e \cup \partial B_e$, $\cup_e \bar{B}_e = \bar{B}$. The intersection, if any, between ∂B_e and a part of ∂B is denoted by ∂B_{ue}, ∂B_{te}, ∂B_{Te}, ∂B_{qe} and ∂B_{ce}, in accordance with the relevant part of ∂B. The interdomain between two contiguous subdomains is denoted by $\rho_j, j=1,\ldots,N$.

On the generic interdomain, the continuity is relaxed for tractions and heat flux, and the temperature is defined independently of the temperature on the adjacent subdomains. Then, statement (16) becomes

$$\int_I \sum_e \delta[\Pi^E_e(\mathbf{u},\boldsymbol{\sigma}) + \tilde{\Pi}^T_e(T,\mathbf{q},\tilde{T},\tilde{q})]\,\mathrm{d}t + \int_I \sum_e G_e\,\mathrm{d}t - \sum_e C_{0e} = 0 \qquad \forall(\delta\mathbf{u},\delta\boldsymbol{\sigma},\delta T,\delta\mathbf{q},\delta\tilde{T},\delta\tilde{q}), \tag{22}$$

where Π^E_e, G_e and C_{0e} are the specialization of expressions (17), (19), (20) to the eth subdomain, and

$$\tilde{\Pi}^T_e(T,\mathbf{q},\tilde{T},\tilde{q}) = -\frac{1}{2}\int_{B_e}\mathbf{q}\cdot\mathbf{k}^{-1}\mathbf{q}\,\mathrm{d}V + \int_{B_e}T(\mathrm{div}\,\mathbf{q}-\gamma)\,\mathrm{d}V - \int_{\partial B_e}\tilde{T}\mathbf{q}\cdot\mathbf{n}\,\mathrm{d}S + \int_{\partial B_{Te}}(\tilde{T}-\bar{T})\tilde{q}\,\mathrm{d}S + \int_{\partial B_{qe}}\tilde{T}\bar{q}\,\mathrm{d}S + \frac{1}{2}\int_{\partial B_{ce}}\kappa(\tilde{T}-T_c)^2\,\mathrm{d}S, \tag{23}$$

where $\tilde{T}(\mathbf{x},t)$ is the temperature on ∂B_e and $\tilde{q}(\mathbf{x},t)$ is a Lagrangian multiplier defined on ∂B_{Te}.

The variation on Π_e^E and $\tilde{\Pi}_e^T$ in statement (22), making use of identities (13) and (14) – see Appendix A –, results for each subdomain B_e in the same field equations and boundary static and kinematic conditions of statement (16), and in the thermal boundary conditions:

$$\tilde{T} - \bar{T} = 0 \quad \text{on } \partial B_{Te}, \tag{24}$$

$$\tilde{q} - \mathbf{q}\cdot\mathbf{n} = 0 \quad \text{on } \partial B_{Te}, \tag{25}$$

$$\mathbf{q}\cdot\mathbf{n} - \bar{q} = 0 \quad \text{on } \partial B_{qe}, \tag{26}$$

$$\mathbf{q}\cdot\mathbf{n} - \kappa(\tilde{T} - T_c) = 0 \quad \text{on } \partial B_{ce}, \tag{27}$$

$$\tilde{T} - T = 0 \quad \text{on } \partial B_e. \tag{28}$$

Moreover, the continuity interdomain conditions for tractions and heat flux are obtained:

$$(\boldsymbol{\sigma}\mathbf{n})_j^+ + (\boldsymbol{\sigma}\mathbf{n})_j^- = \mathbf{0} \quad \text{on } \rho_j,\ j = 1,\ldots,N, \tag{29}$$

$$(\mathbf{q}\cdot\mathbf{n})_j^+ + (\mathbf{q}\cdot\mathbf{n})_j^- = 0 \quad \text{on } \rho_j,\ j = 1,\ldots N. \tag{30}$$

In the following, functions $\boldsymbol{\sigma}$ are assumed to satisfy a priori equilibrium Eq. (5) for each subdomain, and functions $\dot{\boldsymbol{\sigma}}$ are employed in lieu of $\dot{\boldsymbol{\epsilon}}$, via Eq. (10), to express the thermoelastic dissipation. Hence, the functionals

$$\Pi_e^H(\mathbf{u},\boldsymbol{\sigma}) = -\frac{1}{2}\int_{B_e}\boldsymbol{\sigma}\cdot\mathbf{C}^{-1}\boldsymbol{\sigma}\,\mathrm{d}V - \int_{B_e}\boldsymbol{\sigma}\cdot\mathbf{A}(T - T_0)\,\mathrm{d}V + \int_{\partial B_{ue}}\boldsymbol{\sigma}\mathbf{n}\cdot\bar{\mathbf{u}}\,\mathrm{d}S + \int_{\partial B_{te}}(\boldsymbol{\sigma}\mathbf{n} - \bar{\mathbf{t}})\cdot\mathbf{u}\,\mathrm{d}S, \tag{31}$$

$$G_e^H(\boldsymbol{\sigma}, T, \delta T) = \int_{B_e}(T_0\mathbf{A}\cdot\dot{\boldsymbol{\sigma}} + \chi\rho c\dot{T})\delta T\,\mathrm{d}V \tag{32}$$

replace functionals Π_e^E and G_e in Eq. (22), which becomes finally

$$\int_I \sum_e \delta[\Pi_e^H(\mathbf{u},\boldsymbol{\sigma}) + \tilde{\Pi}_e^T(T,\mathbf{q},\tilde{T},\tilde{q})]\,\mathrm{d}t + \int_I \sum_e G_e^H\,\mathrm{d}t - \sum_e C_{0e} = 0 \quad \forall(\delta\mathbf{u},\delta\boldsymbol{\sigma},\delta T,\delta\mathbf{q},\delta\tilde{T},\delta\tilde{q}). \tag{33}$$

Therefore, equilibrium is satisfied strongly and thermal balance expression (15) is met weakly, in B_e. In this way, the variables in B_e are only the functions $\boldsymbol{\sigma}$, T and $\mathbf{q}$, independent for each subdomain, and functions $\mathbf{u}$ and $\tilde{T}$ are defined and continuous on the whole of the interdomains.

4. The mixed model

Functionals (31) and (23) are rewritten in the synthetic form:

$$\Pi_e^{Hr}(\mathbf{u},\boldsymbol{\sigma}) = -\frac{1}{2}\int_{B_e}\boldsymbol{\sigma}\cdot\mathbf{C}^{-1}\boldsymbol{\sigma}\,\mathrm{d}V - \int_{B_e}\boldsymbol{\sigma}\cdot\mathbf{A}(T - T_0)\,\mathrm{d}V + \int_{\partial B_e}\mathbf{u}\cdot(\boldsymbol{\sigma}\mathbf{n} - \mathbf{t})\,\mathrm{d}S, \tag{34}$$

$$\tilde{\Pi}_e^{Tr}(T,\mathbf{q},\tilde{T}) = -\frac{1}{2}\int_{B_e}\mathbf{q}\cdot\mathbf{k}^{-1}\mathbf{q}\,\mathrm{d}V + \int_{B_e}T(\mathrm{div}\,\mathbf{q} - \gamma)\,\mathrm{d}V - \int_{\partial B_e}\tilde{T}(\mathbf{q}\cdot\mathbf{n} - q)\,\mathrm{d}S, \tag{35}$$

where $\mathbf{t}$ and q are, respectively, the traction and the heat flux acting on ∂B_e, to be specialized in accordance with the prescribed conditions for forces and heat flux on ∂B, if present. Boundary conditions on $\mathbf{u}$ and $\tilde{T}$ are not accounted for here, as they are enforced directly, where prescribed on ∂B. Thus, the variational statement (33) for the generic subdomain B_e can be rewritten as

$$\int_I \delta\left(\Pi_e^{Hr} + \tilde{\Pi}_e^{Tr}\right) \mathrm{d}t + \int_I G_e^H \,\mathrm{d}t - C_{0e} = 0 \quad \forall(\delta\mathbf{u}, \delta\boldsymbol{\sigma}, \delta T, \delta\mathbf{q}, \delta\tilde{T}), \tag{36}$$

where G_e^H and C_{0e} are given by Eqs. (32) and (20).

Stress $\boldsymbol{\sigma}$ is formally split as follows:

$$\boldsymbol{\sigma} = \boldsymbol{\sigma}_p + \boldsymbol{\sigma}_h, \tag{37}$$

$$\operatorname{div}\boldsymbol{\sigma}_p = -\mathbf{p}, \tag{38}$$

$$\operatorname{div}\boldsymbol{\sigma}_h = \mathbf{0}, \tag{39}$$

and heat flux $\mathbf{q}$ is analogously split as

$$\mathbf{q} = \mathbf{q}_\gamma + \mathbf{q}_t + \mathbf{q}_h, \tag{40}$$

$$\operatorname{div}\mathbf{q}_\gamma = \gamma, \tag{41}$$

$$\operatorname{div}\mathbf{q}_h = 0, \tag{42}$$

where $\boldsymbol{\sigma}_p$ and $\mathbf{q}_\gamma$ are particular integrals of Eqs. (5) and (6), respectively, $\boldsymbol{\sigma}_h$ and $\mathbf{q}_h$ are indeterminate null-divergence fields, and $\mathbf{q}_t$ is an indeterminate field which is introduced to offset the rate dependent terms in transient conditions, Eq. (15). Hence, functional (35) reduces to

$$\tilde{\Pi}_e^{Tr}(T, \mathbf{q}, \tilde{T}) = -\frac{1}{2}\int_{B_e} \mathbf{q}\cdot\mathbf{k}^{-1}\mathbf{q}\,\mathrm{d}V + \int_{B_e} T\operatorname{div}\mathbf{q}_t\,\mathrm{d}V - \int_{\partial B_e} \tilde{T}(\mathbf{q}\cdot\mathbf{n} - q)\,\mathrm{d}S, \tag{43}$$

and the model is of mixed type as Eq. (15) is met weakly. If the model is applied to stationary thermoelastic problems, then the term $\mathbf{q}_t$ can be dropped and the model becomes of hybrid type (Pian, 1973; Cannarozzi et al., 2000), on the whole.

In the following, the standard matrix notation is employed. Each function dependent on space and time will be expressed as product of a function of $\mathbf{x}$ alone and a function of t alone.

Stress, heat flux and temperature in a subdomain B_e are represented as follows:

$$\boldsymbol{\sigma}_h(\mathbf{x}, t) = \mathbf{P}_h(\mathbf{x})\boldsymbol{\beta}_h(t), \quad \mathbf{q}_h(\mathbf{x}, t) = \mathbf{L}_h(\mathbf{x})\boldsymbol{\psi}_h(t), \quad \mathbf{q}_t(\mathbf{x}, t) = \mathbf{L}_t(\mathbf{x})\boldsymbol{\psi}_t(t), \tag{44}$$

$$T(\mathbf{x}, t) = \mathbf{N}_T(\mathbf{x})\boldsymbol{\tau}(t), \tag{45}$$

where $\mathbf{P}_h$, $\mathbf{L}_h$, $\mathbf{L}_t$ and $\mathbf{N}_T$ are matrices of basis functions and the vectors of indeterminate amplitudes $\boldsymbol{\beta}_h$, $\boldsymbol{\psi}_h$, $\boldsymbol{\psi}_t$ and $\boldsymbol{\tau}$ are inner variables for B_e.

Displacement and temperature on ∂B_e are represented as follows

$$\mathbf{u}(\mathbf{x}, t) = \mathbf{N}_u(\mathbf{x})\mathbf{v}(t), \quad \tilde{T}(\mathbf{x}, t) = \mathbf{N}_{\tilde{T}}(\mathbf{x})\tilde{\boldsymbol{\tau}}(t), \tag{46}$$

where $\mathbf{N}_u$ and $\mathbf{N}_{\tilde{T}}$ are again matrices of basis functions, and $\mathbf{v}$ and $\tilde{\boldsymbol{\tau}}$ are vectors of indeterminate amplitudes and constitute the interdomain variables for the model.

With the above assumptions, the variational statement (36) specializes as follows:

$$\int_I \begin{Vmatrix} \delta\boldsymbol{\beta}_h \\ \delta\boldsymbol{\psi}_{ht} \\ \delta\mathbf{v} \\ \delta\tilde{\boldsymbol{\tau}} \\ \delta\boldsymbol{\tau} \end{Vmatrix}^{\mathrm{T}} \left(\begin{vmatrix} \mathbf{H}_\beta & \mathbf{0} & -\mathbf{G}_v^{\mathrm{T}} & 0 & \boldsymbol{\Lambda} \\ \mathbf{0} & \mathbf{H}_\psi & \mathbf{0} & \mathbf{G}_{\tilde{\tau}}^{\mathrm{T}} & -\mathbf{G}_\tau^{\mathrm{T}} \\ \mathbf{G}_v & \mathbf{0} & \mathbf{0} & \mathbf{0} & \mathbf{0} \\ \mathbf{0} & \mathbf{G}_{\tilde{\tau}} & \mathbf{0} & \mathbf{0} & \mathbf{0} \\ \mathbf{0} & \mathbf{G}_\tau & \mathbf{0} & \mathbf{0} & \mathbf{0} \end{vmatrix} \begin{Vmatrix} \boldsymbol{\beta}_h \\ \boldsymbol{\psi}_{ht} \\ \mathbf{v} \\ \tilde{\boldsymbol{\tau}} \\ \boldsymbol{\tau} \end{Vmatrix} + \begin{Vmatrix} \mathbf{g}_\beta \\ \mathbf{g}_\psi \\ \mathbf{g}_v \\ \mathbf{g}_{\tilde{\tau}} \\ \mathbf{0} \end{Vmatrix} - \begin{Vmatrix} \mathbf{0} \\ \mathbf{0} \\ \mathbf{h}_v \\ \mathbf{h}_{\tilde{\tau}} \\ \mathbf{0} \end{Vmatrix} \right) \mathrm{d}t$$

$$+ \int_I \delta\boldsymbol{\tau}^{\mathrm{T}}(T_0\boldsymbol{\Lambda}^{\mathrm{T}}\dot{\boldsymbol{\beta}}_h + \hat{\mathbf{W}}\dot{\boldsymbol{\tau}})\,\mathrm{d}t - \delta\boldsymbol{\tau}^{\mathrm{T}}\big|_0(\mathbf{W}\boldsymbol{\tau}|_0 - \boldsymbol{\tau}_0) = 0 \qquad \forall(\delta\boldsymbol{\beta}_h, \delta\boldsymbol{\psi}_{ht}, \delta\mathbf{v}, \delta\tilde{\boldsymbol{\tau}}, \delta\boldsymbol{\tau}). \tag{47}$$

All the expressions of matrices and vectors in the above equation are given in Appendix B (I). In the first term, vector $\boldsymbol{\psi}_{ht}$ collects the heat flux parameters $\boldsymbol{\psi}_h$ and $\boldsymbol{\psi}_t$, and vectors $\mathbf{h}_v$ and $\mathbf{h}_{\tilde{\tau}}$ are the (definition of the) generalized nodal forces and nodal heat fluxes, respectively. Matrices $\mathbf{H}_\beta$ and $\mathbf{H}_\psi$, symmetric and positive definite, are the compliance and resistivity matrices of the model, and matrices $\mathbf{G}_v$ and $\mathbf{G}_{\tilde{\tau}}$, $\mathbf{G}_\tau$ are static load and thermal load connection matrices, respectively. Matrix $\boldsymbol{\Lambda}$ accounts for the strain due to temperature as well as for the thermoelastic dissipation (second term) and introduces asymmetry in the whole coefficient matrix, due to coupling. Vectors $\mathbf{g}_\beta$, $\mathbf{g}_v$ and $\mathbf{g}_\psi$, $\mathbf{g}_{\tilde{\tau}}$ collect known nodal quantities due to the distributed thermal and static quantities given in B_e. In the second and third terms, $\hat{\mathbf{W}}$ and $\mathbf{W}$ are symmetric, positive definite matrices, and $\mathbf{W}$ represents the thermal inertia matrix of the model.

Imposing that the variational statement (47) is fulfilled for each $\delta\boldsymbol{\beta}_h$ and $\delta\boldsymbol{\psi}_{ht}$ with $\delta\mathbf{v} = \delta\tilde{\boldsymbol{\tau}} = \delta\boldsymbol{\tau} = \delta\boldsymbol{\tau}|_0 = 0$ leads to the compatibility equations of the model by which the inner variables $\boldsymbol{\beta}_h$ and $\boldsymbol{\psi}_{ht}$ are eliminated. The resulting variational statement reads as

$$\begin{aligned}&\int_I \begin{vmatrix}\delta\mathbf{v}\\ \delta\tilde{\boldsymbol{\tau}}\\ \delta\boldsymbol{\tau}\end{vmatrix}^{\mathrm{T}} \left(\begin{vmatrix}\mathbf{K}_v & \mathbf{0} & -\mathbf{K}_{v\tau}\\ \mathbf{0} & -\mathbf{K}_{\tilde{\tau}} & \mathbf{K}_{\tilde{\tau}\tau}\\ \mathbf{0} & -\mathbf{K}_{\tilde{\tau}\tau}^{\mathrm{T}} & \mathbf{K}_\tau\end{vmatrix} \begin{vmatrix}\mathbf{v}\\ \tilde{\boldsymbol{\tau}}\\ \boldsymbol{\tau}\end{vmatrix} + \begin{vmatrix}\mathbf{p}_v\\ \mathbf{p}_{\tilde{\tau}}\\ \mathbf{p}_\tau\end{vmatrix} - \begin{vmatrix}\mathbf{h}_v\\ \mathbf{h}_{\tilde{\tau}}\\ \mathbf{0}\end{vmatrix} \right) \mathrm{d}t\\ &+ \int_I \delta\boldsymbol{\tau}^{\mathrm{T}}(T_0\mathbf{K}_{v\tau}^{\mathrm{T}}\dot{\mathbf{v}} + \mathbf{M}_\tau\dot{\tilde{\boldsymbol{\tau}}})\,\mathrm{d}t - \delta\boldsymbol{\tau}^{\mathrm{T}}\big|_0(\mathbf{W}\boldsymbol{\tau}|_0 - \boldsymbol{\tau}_0) = 0 \quad \forall(\delta\mathbf{v}, \delta\tilde{\boldsymbol{\tau}}, \delta\boldsymbol{\tau}),\end{aligned} \tag{48}$$

where the definitions of matrices and vectors are given in Appendix B (II). Condition (48) yields the coupled relation between generalized nodal forces/heat fluxes and nodal displacements/temperatures, i.e. the elemental equilibrium/thermal balance equations, and the initial conditions:

$$\begin{vmatrix}\mathbf{h}_v\\ \mathbf{h}_{\tilde{\tau}}\\ \mathbf{0}\end{vmatrix} = \begin{vmatrix}\mathbf{0} & \mathbf{0} & \mathbf{0}\\ \mathbf{0} & \mathbf{0} & \mathbf{0}\\ T_0\mathbf{K}_{v\tau}^{\mathrm{T}} & \mathbf{0} & \mathbf{M}_\tau\end{vmatrix} \begin{vmatrix}\dot{\mathbf{v}}\\ \dot{\tilde{\boldsymbol{\tau}}}\\ \dot{\boldsymbol{\tau}}\end{vmatrix} + \begin{vmatrix}\mathbf{K}_v & \mathbf{0} & -\mathbf{K}_{v\tau}\\ \mathbf{0} & -\mathbf{K}_{\tilde{\tau}} & \mathbf{K}_{\tilde{\tau}\tau}\\ \mathbf{0} & -\mathbf{K}_{\tilde{\tau}\tau}^{\mathrm{T}} & \mathbf{K}_\tau\end{vmatrix} \begin{vmatrix}\mathbf{v}\\ \tilde{\boldsymbol{\tau}}\\ \boldsymbol{\tau}\end{vmatrix} + \begin{vmatrix}\mathbf{p}_v\\ \mathbf{p}_{\tilde{\tau}}\\ \mathbf{p}_\tau\end{vmatrix}, \tag{49}$$

$$\mathbf{W}\boldsymbol{\tau}|_0 - \boldsymbol{\tau}_0 = \mathbf{0}, \tag{50}$$

respectively.

Following the standard finite element procedure (Zienkiewicz and Taylor, 1989), the nodal equilibrium and thermal balance equations can be assembled starting from Eq. (49) and the displacement and temperature boundary conditions are subsequently enforced.

Eq. (48) is the starting point for variationally based time integration methods in thermoelastic analysis, where temperature and displacement parameters are discretized in the time domain (Ubertini, 1998; Mancuso et al., 1998). On the other hand, the differential Eq. (49), with the initial condition (50), is the basis for the thermoelastic analysis by finite difference time integration methods (Hughes, 1987). Both variational and finite difference time integration methods can be implemented using a staggered or a monolithic solution scheme (Wood, 1990).

5. A finite element implementation

In this section, a finite element scheme of representation in the space domain is derived from the proposed model, the related properties of stability, consistency and invariance are investigated, and some aspects concerning the computational burden are discussed.

Elemental matrices and vectors are conveniently computed working in a local (element) reference system $(O;\bar{x}_i)$ and using a local node numbering – see Fig. 1 for the bidimensional case. The element geometry is described by means of a parametric representation, as usual in the finite element approach. The displacement $\mathbf{u}$ and the interelement temperature $\tilde{T}$ are represented, according to Eq. (46), in terms of nodal

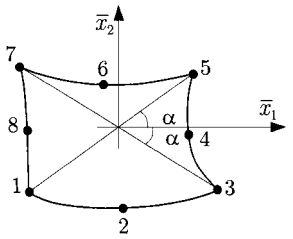

Fig. 1. Local reference system and node numbering for the bidimensional case.

values and shape functions defined onto the natural domain (master element), with nodes placed on the element boundary. The inner temperature T can be represented by means of algebraic functions defined onto either the physical or the natural domain, as T is a variable internal to each element. For a coherent assumption, the representation assumed for T should match the one for $\tilde{T}$ on the element boundary, in the sense that they would have the same number of free parameters on the element boundary – hierarchical representation of T (Zienkiewicz and Taylor, 1989).

The null-divergence stress field $\boldsymbol{\sigma}_h$ and heat flux field $\mathbf{q}_h$ can be deduced from algebraic stress and stream functions, $\Phi(\bar{\mathbf{x}})$ and $\omega(\bar{\mathbf{x}})$, defined in the local reference system, as follows (subscript $/_i$ denotes differentiation with respect to $\bar{x}_i$):

bidimensional case

$$\boldsymbol{\sigma}_h^{\mathrm{T}} = |\,\sigma_{h11} \quad \sigma_{h22} \quad \sigma_{h12}\,|, \qquad \mathbf{q}_h^{\mathrm{T}} = |\,q_{h1} \quad q_{h2}\,|,$$
$$\sigma_{h11} = \Phi_{/2,2}, \quad \sigma_{h22} = \Phi_{/1,1}, \quad \sigma_{h12} = -\Phi_{/1,2}, \tag{51}$$

$$q_{h1} = \omega_{/2}, \quad q_{h2} = -\omega_{/1}, \tag{52}$$

tridimensional case

$$\boldsymbol{\sigma}_h^{\mathrm{T}} = |\,\sigma_{h11} \quad \sigma_{h22} \quad \sigma_{h33} \quad \sigma_{h23} \quad \sigma_{h13} \quad \sigma_{h12}\,|, \qquad \mathbf{q}_h^{\mathrm{T}} = |\,q_{h1} \quad q_{h2} \quad q_{h3}\,|,$$
$$\sigma_{h11} = \Phi_{1/2,3}, \quad \sigma_{h22} = \Phi_{2/1,3}, \quad \sigma_{h33} = \Phi_{3/1,2}, \tag{53}$$

$$\sigma_{h12} = \Phi_{3/3,3}, \quad \sigma_{h13} = \Phi_{2/2,2}, \quad \sigma_{h23} = \Phi_{1/1,1}, \tag{54}$$

$$q_{h1} = \omega_{1/2,3}, \quad q_{h2} = \omega_{2/1,3}, \quad q_{h3} = \omega_{3/1,2} \tag{55}$$

under the constraints

$$\Phi_{1/1} + \Phi_{2/2} + \Phi_{3/3} = 0, \qquad \omega_1 + \omega_2 + \omega_3 = 0.$$

It can be easily verified that both the above sets of assumptions fulfill conditions (39) and (42), respectively. The stress function scheme for the tridimensional case was proposed by Zanaboni (1936).

The representation of $\mathbf{q}_t$ is developed with the aim of offsetting both the rate dependent terms, according to

$$\operatorname{div}\mathbf{q}_t = -T_0\mathbf{A}\cdot\dot{\boldsymbol{\sigma}}_h - \chi\rho c\dot{T}, \tag{56}$$

which is obtained by substituting Eqs. (40) and (37) into Eq. (15). For this purpose, the representation of $\mathbf{q}_t$ is directly related to the one of stress $\boldsymbol{\sigma}_h$ by requiring that the space of $\operatorname{div}\mathbf{q}_t$ coincides with the space of the stress rate term $T_0\mathbf{A}\cdot\dot{\boldsymbol{\sigma}}_h$, in accordance with the following scheme:

bidimensional case

$$\mathbf{q}_t^{\mathrm{T}} = |\,q_{t1} \quad q_{t2}\,|, \qquad \mathbf{A}^{\mathrm{T}} = |\,\alpha_{11} \quad \alpha_{22} \quad 2\alpha_{12}\,|, \qquad q_{t1} = \alpha_{22}\Phi_{/1} - \alpha_{12}\Phi_{/2}, \quad q_{t2} = \alpha_{11}\Phi_{/2} - \alpha_{12}\Phi_{/1}, \tag{57}$$

tridimensional case

$$\mathbf{q}_t^{\mathrm{T}} = |\, q_{t1} \quad q_{t2} \quad q_{t3} \,|, \qquad \mathbf{A}^{\mathrm{T}} = |\, \alpha_{11} \quad \alpha_{22} \quad \alpha_{33} \quad 2\alpha_{23} \quad 2\alpha_{13} \quad 2\alpha_{12} \,|, \tag{58}$$

$$q_{t1} = \tfrac{1}{2}(\alpha_{22}\Phi_{2/1,3} + \alpha_{33}\Phi_{3/1,2}) + 2\alpha_{23}\Phi_{1/1,1}, \tag{59}$$

$$q_{t2} = \tfrac{1}{2}(\alpha_{11}\Phi_{1/2,3} + \alpha_{33}\Phi_{3/1,2}) + 2\alpha_{13}\Phi_{2/2,2}, \tag{60}$$

$$q_{t3} = \tfrac{1}{2}(\alpha_{11}\Phi_{1/2,3} + \alpha_{22}\Phi_{2/1,3}) + 2\alpha_{12}\Phi_{3/3,3}. \tag{61}$$

In this way, the representation of $\mathbf{q}_t$ in the space domain stems directly from the assumed stress functions. Note that only the modes of $\mathbf{q}_t$ linearly independent from those assumed for $\mathbf{q}_h$ should be retained in the above representations, in order to avoid singularity in the resistivity matrix $\mathbf{H}_\psi$.

For the purpose of element stability, stress and stream functions are to be selected, so that no (kinematic or thermal) spurious or zero energy modes arise, i.e. so that the elemental stiffness and conductivity matrices are rank sufficient. The stability condition for finite element models based on a general multi-variable variational approach has been investigated (Xue and Atluri, 1985) based on the Babuska–Brezzi condition (e.g. Brezzi and Fortin, 1991). For the present model, the necessary conditions for the absence of a zero energy mode can be expressed explicitly as

$$n_{sh} \geqslant n_u - n_r, \tag{62}$$

$$n_{qh} + n_{q_t} \geqslant n_T + n_{\tilde{T}} - 1, \tag{63}$$

where n_{sh}, n_u, n_{qh}, n_{qt}, n_T and $n_{\tilde{T}}$ are respectively the number of parameters in the representations of $\boldsymbol{\sigma}_h$, $\mathbf{u}$, $\mathbf{q}_h$, $\mathbf{q}_t$, T and $\tilde{T}$, n_r is the number of the element rigid body motions, and number 1 in Eq. (63) stands for the constant temperature distribution which is admitted without heat strain. As a consequence, once the displacement and temperature representations are assumed, the minimum number of stress and flux parameters are determined. It is evident that the smaller the value of n_{sh} and $(n_{qh} + n_{q_t})$, the lower is the computing cost for eliminating stress and heat flux parameters at the element level. Moreover, a better performance is expected if the number of stress and heat flux modes is equal or close to the value determined by Eqs. (62) and (63), respectively. In fact, a large number of assumed stress modes could lead to increased stiffness (Pian, 1973), and the same consideration holds for heat flux.

For a coherent implementation, the consistency between the spatial representations of mechanical and thermal variables should be considered; otherwise, inaccurate results and unreliable stress predictions could be obtained (Prathap and Naganarayana, 1995). The second term in functional (34) expresses the work done by the stress on the strain due to temperature (thermal strain). This term leads to matrix $\boldsymbol{\Lambda}$ and once stress and heat flux parameters are condensed out, to the thermoelastic coupling matrix $\mathbf{K}_{v\tau}$. Then, the compatibility equations of the model correctly reflect the assumed temperature representation, if the assumed stress representation works on the whole thermal strain. In fact, only the part of the thermal strain on which the stress does work is actually sensed by the solution in terms of both displacements and stresses. As a consequence, the representation space of each stress component should include the representation space of the corresponding thermal strain component, as a necessary requirement for the consistency of the model (de Miranda and Ubertini, 1999). In this way, the temperature enters properly in the computation of matrix $\boldsymbol{\Lambda}$. Moreover, if the assumed stress modes are not energy-orthogonal to any strain modes – in the sense of the work integral expressed by the third term in Eq. (34) – the above condition is also sufficient to prevent from spurious outcomes in the stress recovery. In fact, this further requirement on stress assumptions secures that all thermal modes actually participates in computing the coupling matrix $\mathbf{K}_{v\tau}$. Therefore, the representations of stress $\boldsymbol{\sigma}_h$, displacement $\mathbf{u}$ and temperature T should be matched according to the above consistency condition, and if the number of stress modes is close or equal to the number of strain modes, then the best behaviour is expected. Consistency condition is to be clearly verified onto the physical domain. As a consequence, element geometry distortions can provoke loss of consistency, if the

temperature T is defined onto the natural domain. In fact, owing to the coordinate transformation, the resulting representation in the physical domain is generally no more fully algebraic (e.g. Cannarozzi and Mondelli, 1998), and consistency is restricted to the algebraic part only. Obviously, the loss of consistency does not occur, if the temperature T is directly defined onto the physical domain. Based on the considerations about consistency, the reason why inner and boundary temperatures have been separated appears more clearly. In fact, the improvement in the thermal response is obtained through a more flexible representation of temperature, without acting on the degree of its representation and without affecting the consistency with the stress representation. Finally, it is worthwhile to note that if the consistency condition is met and the representation of $\mathbf{q}_t$ is obtained from stress functions as previously described, then the function space of $\operatorname{div}\mathbf{q}_t$ in the spatial domain coincides with the one of the whole right-hand side in Eq. (56).

A further condition to be satisfied is the invariance of the model with respect to any coordinate change, in the sense that implementing it in the local system of coordinates or, alternatively, in the global one should lead to the same result (Sze et al., 1992). This requirement secures that the finite element implementation is independent of the local system adopted. The interelement displacement and temperature, $\mathbf{v}$ and $\tilde{\tau}$, the stress $\boldsymbol{\sigma}_p$, and the heat flux $\mathbf{q}_\gamma$ meet invariance as well as the inner temperature T if defined onto the natural domain. With regard to $\boldsymbol{\sigma}_h$, $\mathbf{q}_h$ and $\mathbf{q}_t$ as well as to T if defined directly in terms of the local coordinates, element invariance is met if complete representations are assumed. In fact, completeness secures that a polynomial basis does not change under a linear transformation of coordinates, i.e. by changing the reference coordinate frame. For stress and heat flux, this is obtained by assuming complete stress and stream functions. Some considerations about the relative invariance can be added. If a representation is of degree g but complete up to degree $g-1$, then only invariance with respect to translation of axes is retained. In general, invariance is kept for the modes up to the maximum degree of completeness. In the bidimensional case, if a representation is invariant with respect to a $\pi/2$ rotation of the reference axes, then, invariance with respect to node numbering is kept, due to the local reference system adopted, Fig. 1.

Finally, some attention deserves the computational issue. Unlike standard compatible finite elements, an extra computational cost for eliminating stress and heat flux parameters is required. Moreover, both the global vectors of temperature degrees of freedom, say $\tilde{\boldsymbol{\tau}}_g$ and $\boldsymbol{\tau}_g$, as well as the global vector of displacement degrees of freedom, say $\mathbf{v}_g$, are unknown in the semidiscrete system of equations. As can be observed, the interelement temperatures $\tilde{\boldsymbol{\tau}}_g$ and displacement $\mathbf{v}_g$ can be obtained directly in terms of $\boldsymbol{\tau}_g$ as

$$\mathbf{v}_g = \mathbf{K}_v^{-1}(\mathbf{K}_{v\tau}\boldsymbol{\tau}_g - \mathbf{p}_v), \qquad \tilde{\boldsymbol{\tau}}_g = -\mathbf{K}_{\tilde{\tau}}^{-1}(\mathbf{K}_{\tilde{\tau}\tau}\boldsymbol{\tau}_g + \mathbf{p}_{\tilde{\tau}}), \tag{64}$$

where matrices and vectors are to be intended as assembled and the boundary conditions applied. Substituting these expressions into the remaining equation yields

$$\bar{\mathbf{M}}_\tau\dot{\boldsymbol{\tau}}_g + \bar{\mathbf{K}}_\tau\boldsymbol{\tau}_g + \bar{\mathbf{p}}_\tau = \mathbf{0}, \tag{65}$$

where

$$\bar{\mathbf{K}}_\tau = \mathbf{K}_\tau + \mathbf{K}_{\tilde{\tau}\tau}^{\mathrm{T}}\mathbf{K}_{\tilde{\tau}}^{-1}\mathbf{K}_{\tilde{\tau}\tau}, \quad \bar{\mathbf{p}}_\tau = \mathbf{p}_\tau + \mathbf{K}_{\tilde{\tau}\tau}^{\mathrm{T}}\mathbf{K}_{\tilde{\tau}}^{-1}\mathbf{p}_{\tilde{\tau}}, \quad \bar{\mathbf{M}}_\tau = \mathbf{M}_\tau + T_0\mathbf{K}_{v\tau}^{\mathrm{T}}\mathbf{K}_v^{-1}\mathbf{K}_{v\tau}.$$

Matrices $\bar{\mathbf{K}}_\tau$ and $\bar{\mathbf{M}}_\tau$ are symmetric and positive definite and $\bar{\mathbf{M}}_\tau$ represents a modified capacity matrix due to the thermoelastic dissipation. It emerges that, although heavy, eliminating the interelement degrees of freedom could be convenient. In fact, time integration can be carried out in Eq. (65) instead of on the whole assembly. Moreover, standard implementation of direct time integration algorithms as well as modal decomposition procedure can be applied due to the symmetric and standard form of Eq. (65). From the authors' experience, the better accuracy of the mixed model offsets in general the computational burden, as is shown in the following through some numerical tests.

6. Numerical tests

The guidelines exposed in Section 5 have been applied to develop three plane, quadrilateral, parametric finite elements, described in the following. The assumed stress and heat flux representations are given in Appendix C.

Element M44. Displacement and temperature $\tilde{T}$ are represented on each side by linear shape functions ($n_u = 2 \times 4$ and $n_{\tilde{T}} = 4$), based on corner nodes (four-node scheme), and inner temperature T is represented by bilinear functions defined onto the natural domain ($n_t = 4$). Stress field $\boldsymbol{\sigma}_h$ and heat flux field $\mathbf{q}_h$ are obtained via Eqs. (51) and (52) from a cubic stress function Φ ($n_{sh} = 7$) and a quadratic stream function ω ($n_{q_h} = 5$). With these assumptions, the element is not stable, as the element conductivity matrix has one spurious mode. In order to stabilize the element, heat flux field $\mathbf{q}_t$ is derived via Eq. (57) using a function $\hat{\Phi}$ obtained by enriching the polynomial basis of function Φ with the monomials $\bar{x}_1^3\bar{x}_2$ and $\bar{x}_1\bar{x}_2^3$ ($n_{q_t} = 7$). Invariance with regard to translation of axes and node numbering is kept, and the assumed stress representation is consistent only with the linear part of the temperature representation. Anyway, spurious outcomes in the stress recovery are prevented and the function space of $\operatorname{div}\mathbf{q}_t$ still coincides with the one of the rate dependent terms in regular geometry. Notice that for steady state analysis, the element can be also used in the hybrid version, which is obtained by dropping the heat flux $\mathbf{q}_t$ and the inner temperature T. For computing the coupling matrix Λ, the element interior temperature distribution is interpolated by taking the bilinear shape functions corresponding to the assumed representation for $\tilde{T}$ on the element boundary. In this version, the element is invariant, as well as stable and consistent with the linear part of the temperature representation, and the stress recovery is still free from spurious outcomes.

Element M48. Displacement is represented on each side by quadratic shape functions ($n_u = 2 \times 8$), based on corner and midside nodes (eight-node scheme), whereas temperature $\tilde{T}$ is represented on each side by linear shape functions ($n_{\tilde{T}} = 4$), based on corner nodes (four-node scheme). Inner temperature T is represented by bilinear functions defined onto the natural domain ($n_t = 4$). Stress field $\boldsymbol{\sigma}_h$ and heat flux field $\mathbf{q}_h$ are obtained via Eqs. (51) and (52) from a quintic stress function Φ ($n_{sh} = 18$) and a quadratic stream function ω ($n_{q_h} = 5$), and the representation of heat flux $\mathbf{q}_t$ is obtained according to Eq. (57) ($n_{q_t} = 16$). With these assumptions, the element is stable, fully consistent in regular geometry and invariant, but the resulting number of flux parameters appears to be too large with respect to the minimum number dictated by Eq. (63). With regard to steady state analysis, the hybrid version of M48 can be implemented in the same manner of M44, and the resulting element is still stable, fully consistent in regular geometry and invariant.

Element M88. Displacement and temperature $\tilde{T}$ are represented on each side by quadratic shape functions ($n_u = 2 \times 8$ and $n_{\tilde{T}} = 8$), based on corner and midside nodes (eight-node scheme), and inner temperature T is represented by quadratic serendipity functions defined onto the natural domain ($n_t = 8$). Stress field $\boldsymbol{\sigma}_h$ and heat flux field $\mathbf{q}_h$ are obtained via Eqs. (51) and (52) from a quintic stress function Φ ($n_{sh} = 18$) and a quadratic stream function ω ($n_{q_h} = 5$), and the representation of heat flux $\mathbf{q}_t$ is obtained according to Eq. (57) ($n_{q_t} = 16$). With these assumptions, the element is stable, fully consistent in regular geometry and invariant. With regard to steady state analysis, the hybrid version of this element is not stable on the thermal side and a cubic stream function ω is to be used ($n_{q_h} = 9$) (Cannarozzi et al., 2000). Moreover, for computing the coupling matrix $\boldsymbol{\Lambda}$, the element interior temperature distribution is interpolated by taking the quadratic serendipity shape functions corresponding to the assumed representation for $\tilde{T}$ on the element boundary. In this version, the element is still stable, fully consistent in regular geometry and invariant.

Notice that, in the above elements, securing invariance is preferred to secure full consistency in the presence of element distortions, owing to the choice of representing the inner temperature on the natural domain. Alternatively, the above elements can also be implemented by directly defining the representation of T in the local system. In this way, consistency in distorted geometry is retained and invariance is kept

only with regard to translation and node numbering. This second possibility has also been investigated, but it is not further illustrated as the resultant elements exhibit almost the same performance of those described above.

The proposed elements are tested in two reference cases and compared with the usually employed finite elements based on displacement and temperature interpolation. In particular, the results obtained with the following temperature/displacement plane elements are included:

- C44: lagrangian four-node temperature and displacement interpolations,
- C48: lagrangian four-node temperature and serendipity eight-node displacement interpolations,
- C88: serendipity eight-node temperature and displacement interpolations.

Notice that elements C44 and C88 are not consistent, so stresses computed directly from the elastokinematic equations can show extraneous oscillations (Prathap and Naganarayana, 1995), which originate from the mismatch between element strain and strain due to temperature. These spurious outcomes could be mitigated or eliminated resorting to some procedures proposed in the literature, but here no special technique is employed and the stress recovery is performed via the elastokinematic equations, since compatible elements have been included only for comparison.

In the following numerical tests, the interelement and displacement degrees of freedom are eliminated after the semidiscretization and time integration is performed using the modal decomposition procedure (e.g. Hughes, 1987) by exactly integrating each single mode. In this way, the numerical results are free from the errors which would be inevitably introduced by time stepping algorithms, and the performance of the model can be assessed more clearly. The integrals in the mixed model are evaluated using the gaussian quadrature rule. The proper number of quadrature points to evaluate exactly the integrals has been employed. A consistent system of units is assumed.

6.1. Test 1

This case test is derived from Danilovskaya's problem (Danilovskaya, 1950) by suitably modifying the displacement boundary conditions. An elastic isotropic homogeneous layer of thickness L, density ρ, Young's modulus E, Poisson ratio $v = 0.3$, thermal expansion coefficient α, specific heat c, and thermal conductivity k is considered. The layer is initially at the uniform reference temperature T_0, the bottom surface ($x_1 = 0$) is restrained and insulated, and the top surface ($x_1 = L$) is restrained – differently from Danilovskaya's problem. At $t = 0$, the temperature on the top surface is abruptly raised and maintained at the constant value $T_0 + \Delta T$. A measure of the thermoelastic coupling is given by the dimensionless thermoelastic coupling parameter:

$$\delta = \frac{(1+v)\alpha^2 E T_0}{(1-v)(1-2v)\rho c},$$

where $\delta = 0$ corresponds to the uncoupled case. For traditional materials, δ ranges from 0.01 to 0.1. Here, the thermoelastic coupling parameter is assumed as $\delta = 0.5$ (e.g. Carter and Booker, 1989; Tay, 1992), which corresponds to sensible coupling effects, typical of some non-traditional materials, such as certain high-performance composites (Rao and Sinha, 1997).

The problem described is one dimensional and the finite element solutions are obtained using a uniform six-element mesh. The reference solution in terms of displacement, temperature, stress and heat flux is obtained using a uniform finite element mesh, consisting of 100 C88 elements. Indicating with superscript r the reference values and with superscript h the computed values, the local errors are measured by the following normalized quantities:

$$e_{ui} = \frac{(1-\nu)}{(1+\nu)\alpha L\,\Delta T}(u_i^h - u_i^r), \qquad e_T = \frac{1}{\Delta T}(T^h - T^r), \tag{66}$$

$$e_{\sigma ij} = \frac{(1-2\nu)}{\alpha E\,\Delta T}(\sigma_{ij}^h - \sigma_{ij}^r), \qquad e_{qi} = \frac{L}{k\,\Delta T}(q_i^h - q_i^r). \tag{67}$$

The displacement error e_{u1} and the temperature error e_T in A are plotted in Fig. 2 versus the dimensionless time τ, $\tau = (kt)/(\rho c L^2)$. Likewise, the stress error $e_{\sigma 11}$ and the heat flux error e_{q1} in B are plotted in Fig. 3. The results obtained with element C48 by halving the element size have also been included in both the figures. The error values at some significant instants are given in Table 1. To give an idea of the computational effort, Table 2 gives the number of degrees of freedom in the semidiscrete equations obtained with mixed and compatible elements.

As can be clearly observed, mixed elements are considerably more accurate than the compatible ones having the same number of nodes. In particular, the local errors relative to mixed elements are rather uniform and limited even in the initial transient, differently from compatible elements. This reveals a good accuracy also in the higher modes of the semidiscretization, and good predictions are obtained even though a coarse mesh is used. On the other hand, the error curves of compatible elements show that a mesh refinement is required for increasing their accuracy especially in the short term. However, the performance of mixed elements is still better even if compared with the one exhibited by C48 for 12×1 element mesh. It is worth noting that the semidiscretization consisting in 12×1 C48 elements has the largest number of degrees of freedom, on the whole. Moreover, C48 is the element generally employed for thermoelastic analysis owing to its consistency. With regard to the relative performance of mixed elements, M48 appears to be slightly stiff on the thermal side, as the number of flux parameters is much larger than the number of temperature degrees of freedom.

The sensitivity of the mixed model to element geometry distortions is investigated by solving the same problem using a series of six-element meshes with progressively distorted elements, Fig. 4(a). Note that all elements have the same area. The distortion is measured by the parameter φ, which ranges from 0 to $5\pi/12$. The errors are plotted against the distortion parameter in Figs. 4 and 5, at $\tau = 0.25$. Fig. 4 shows the displacement error e_{u1} and the temperature error e_T in A, whereas Fig. 5 shows the stress error $e_{\sigma 11}$ and the

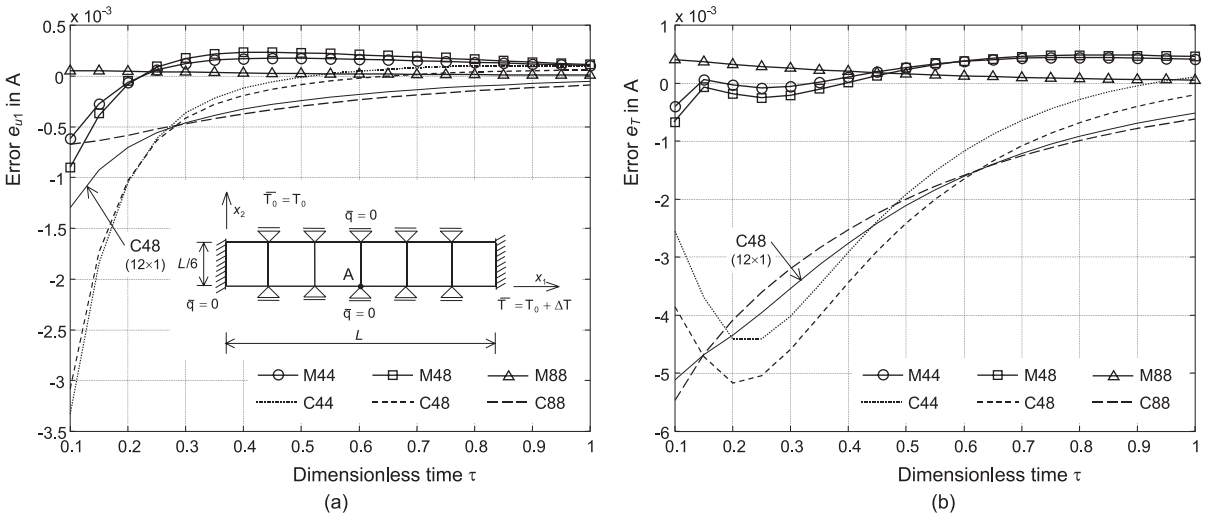

Fig. 2. Test 1 – error time histories in A: (a) displacement u_1 and (b) temperature.

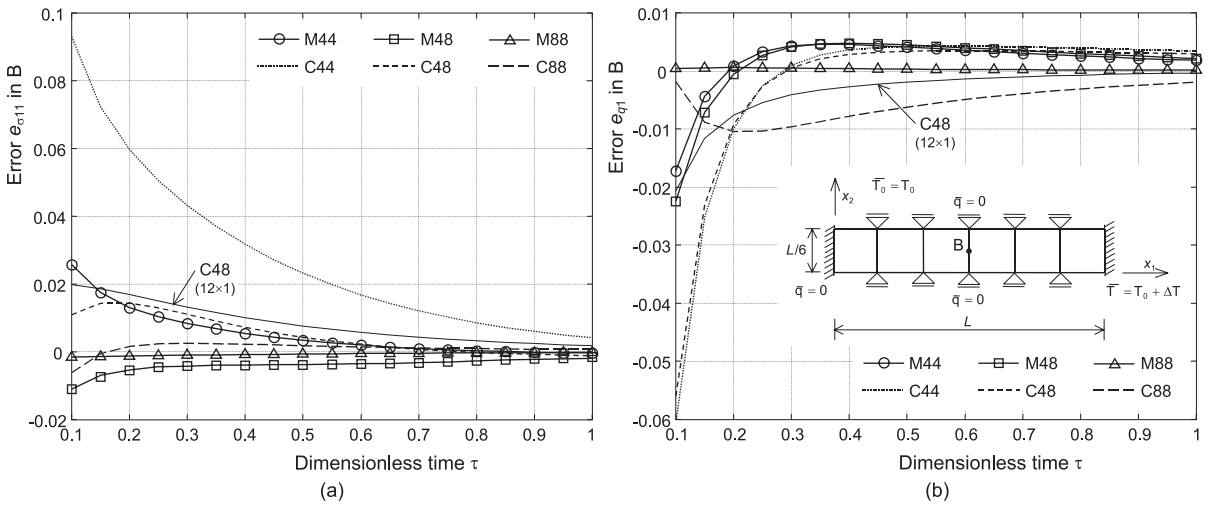

Fig. 3. Test 1 – error time histories in B: (a) normal stress σ_{11} and (b) heat flux q_1.

Table 1
Test 1 – errors in displacement u_1 and temperature in A, and in normal stress σ_{11} and heat flux q_1 in B (see Figs. 2 and 3)

Element	Errors	$\tau = 0.1$	$\tau = 0.3$	$\tau = 0.5$	$\tau = 0.7$	$\tau = 0.9$
M44	$e_{u1} \times 10^{-3}$	−6.1567	1.2455	1.7442	1.5008	1.1864
	$e_T \times 10^{-4}$	−4.0366	−0.3928	2.6771	4.2755	4.3426
	$e_{\sigma 11} \times 10^{-2}$	2.5733	0.8358	0.3404	0.0979	−0.0111
	$e_{q1} \times 10^{-3}$	−17.2183	4.2777	4.0837	3.0229	2.1663
M48	$e_{u1} \times 10^{-4}$	−9.0198	1.7802	2.2408	1.8930	1.2838
	$e_T \times 10^{-4}$	−6.7224	−2.1410	2.7605	4.3322	4.4186
	$e_{\sigma 11} \times 10^{-2}$	−1.0043	−0.3702	−0.3467	−0.2666	−0.1570
	$e_{q1} \times 10^{-3}$	−22.5067	4.1226	4.1855	3.1629	2.2540
M88	$e_{u1} \times 10^{-4}$	0.5175	0.3765	0.2413	0.1522	0.0959
	$e_T \times 10^{-4}$	4.0536	2.5455	1.5903	1.0012	0.6307
	$e_{\sigma 11} \times 10^{-2}$	−0.1572	−0.1007	−0.0633	−0.0399	−0.0251
	$e_{q1} \times 10^{-3}$	0.4266	0.4781	0.3107	0.1960	0.1234
C44	$e_{u1} \times 10^{-4}$	−33.2769	−3.6450	−0.1168	0.7988	1.0255
	$e_T \times 10^{-4}$	−25.5404	−40.2045	−19.1697	−6.4363	−0.4679
	$e_{\sigma 11} \times 10^{-2}$	9.3075	4.3292	2.3224	1.2057	0.5988
	$e_{q1} \times 10^{-3}$	−60.7727	0.5673	3.9702	3.7835	3.3234
C48	$e_{u1} \times 10^{-4}$	−30.7978	−4.1552	−0.8428	0.1569	0.5094
	$e_T \times 10^{-4}$	−38.6050	−45.8564	−24.2124	−10.8205	−3.9904
	$e_{\sigma 11} \times 10^{-2}$	1.0937	1.1108	0.4360	0.0820	−0.0694
	$e_{q1} \times 10^{-3}$	−56.1140	0.4269	3.1755	3.0774	2.7556
C88	$e_{u1} \times 10^{-4}$	−6.7353	−4.6951	−2.9510	−1.8491	−1.1585
	$e_T \times 10^{-4}$	−54.6990	−31.9930	−20.0054	−12.5338	−7.8530
	$e_{\sigma 11} \times 10^{-2}$	−0.6125	0.4482	0.2755	0.1502	0.0689
	$e_{q1} \times 10^{-3}$	−1.8594	−9.6074	−6.2408	−3.9177	−2.4556

Table 2
Test 1 – number of degrees of freedom of the semidiscrete system of equations

Number of degrees of freedom	M44 6×1	M48 6×1	M88 6×1	C44 6×1	C48 6×1	C88 6×1	C48 12×1
Displacement	28	66	66	28	66	66	126
Temperature	24	24	48	14	14	33	26
Total	52	90	114	42	80	99	152

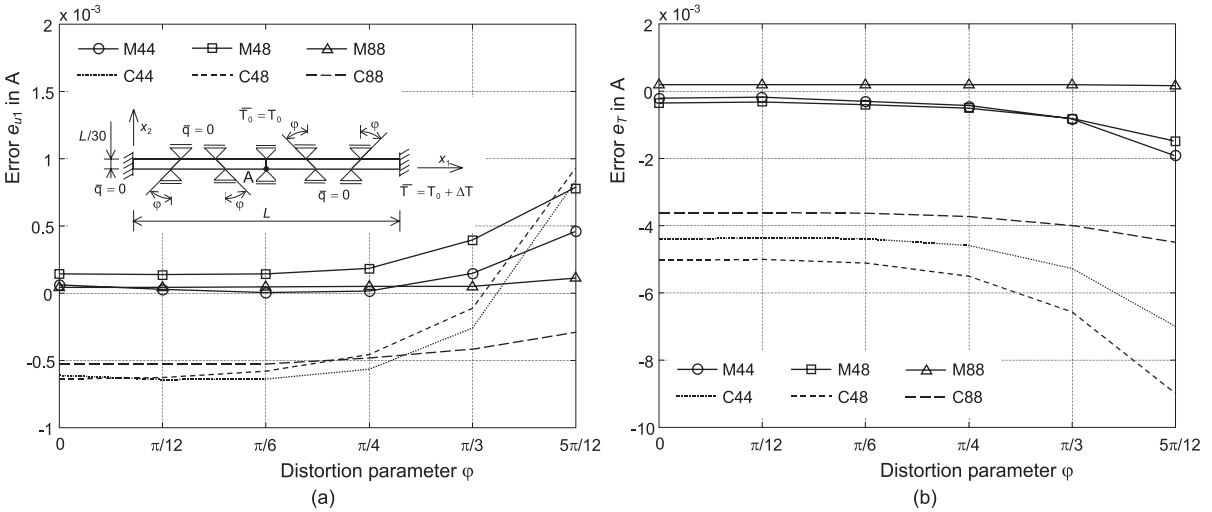

Fig. 4. Sensitivity to geometric distortion, at $\tau = 0.25$: (a) error in displacement u_1 in A and (b) temperature error in A.

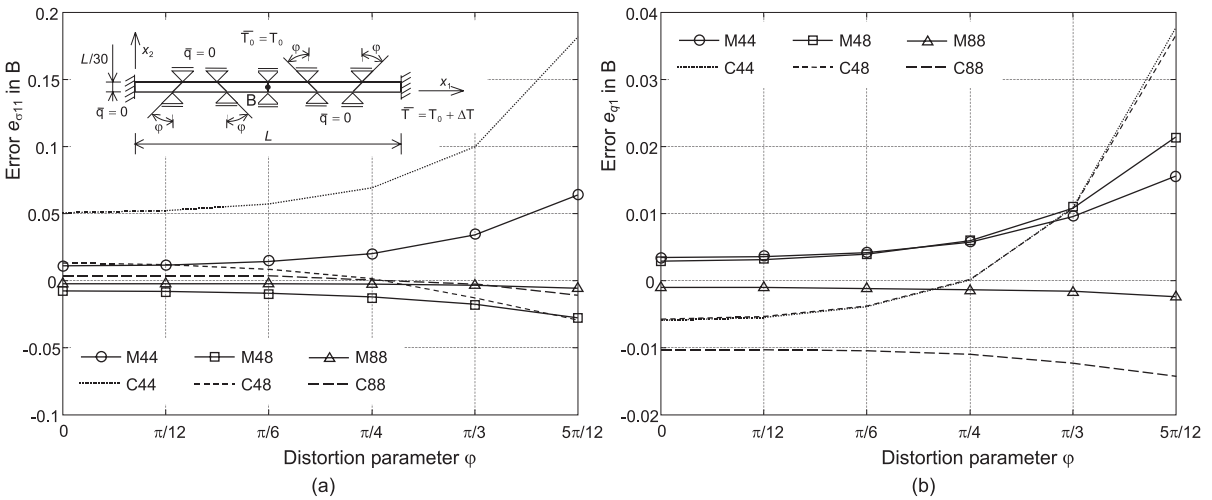

Fig. 5. Sensitivity to geometric distortion, at $\tau = 0.25$: (a) error in normal stress σ_{11} in B and (b) error in heat flux q_1 in B.

heat flux error e_{q2} in C. No tables have been included due to the clarity of the figures. As can be observed, all the errors relative to mixed elements vary only slightly as the distortion parameter increases. On the contrary, compatible elements are much more sensitive to element distortions.

6.2. Test 2

An elastic isotropic homogeneous square plate of side length L, density ρ, Young's modulus E, Poisson ratio $v = 0.3$, thermal expansion coefficient α, specific heat c, and thermal conductivity k is considered. The plate is initially at the uniform reference temperature T_0 and two adjacent sides ($x_1 = 0$ and $x_2 = 0$) are restrained and insulated. At $t = 0$, the temperature on the other two adjacent sides ($x_1 = L$ and $x_2 = L$) is abruptly raised and maintained at the constant value $T_0 + \Delta T$. As in the previous test, the thermoelastic coupling parameter of the material is 0.5. The problem is solved using a uniform 5×5 element mesh and the reference solution is carried out using a uniform mesh with 100 C88 elements per side. The local errors in displacement, temperature, stress and heat flux are measured in accordance with Eqs. (66) and (67).

The time histories of the displacement error e_{u1} in A and the temperature error e_T in B are shown in Fig. 6, whereas the time histories of the stress error $e_{\sigma 22}$ and the heat flux error e_{q2} in C are shown in Fig. 7. Table 3 gives some of the related numerical values. As in the previous test, the numerical response of element C48 obtained by halving the element size of the discretization has been included for a more comprehensive comparison. An indication about the computational cost can be drawn from Table 4, which gives the number of degrees of freedom for various finite element semidiscretizations.

The results qualitatively reflect those of the previous test and confirm the good qualities of the mixed model. In particular, the solutions provided by the mixed elements are in good agreement with the reference solution over all the time range of interest. The relevant errors are much smaller than those of the compatible elements with equal number of nodes, especially in the short term. This confirms the better accuracy of the mixed elements in the higher modes of response, which are of importance in the initial transient. Halving the element size, the accuracy of C48 increases but it is still poor in comparison with M48 and M88, although its larger number of degrees of freedom. On the thermal side, also element M44 is competitive with C48 for 10×10 element mesh, being more accurate in predicting both temperature and heat

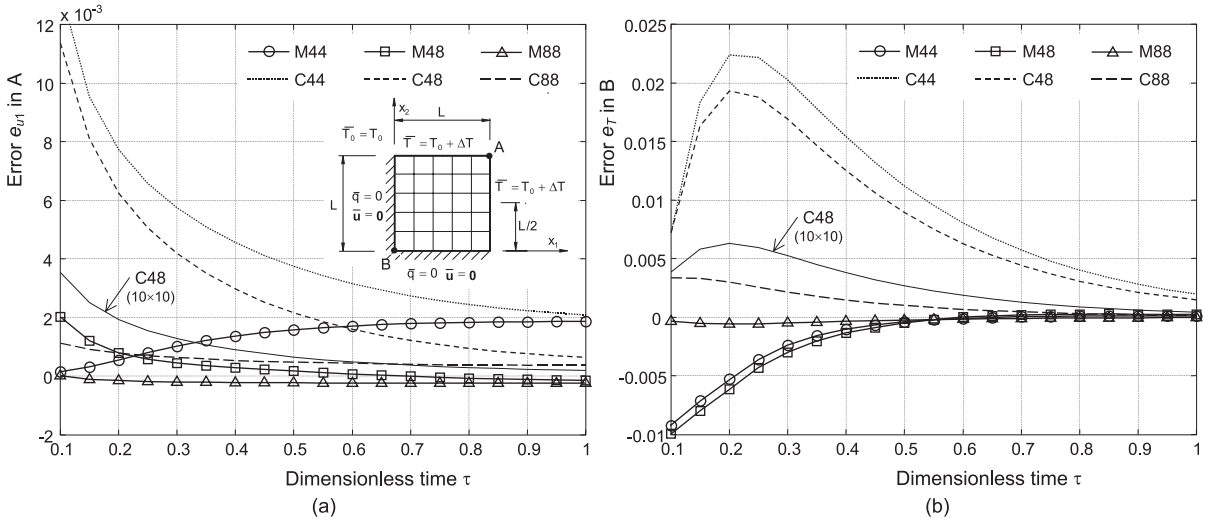

Fig. 6. Test 2 – error time histories: (a) displacement u_1 in A and (b) temperature in B.

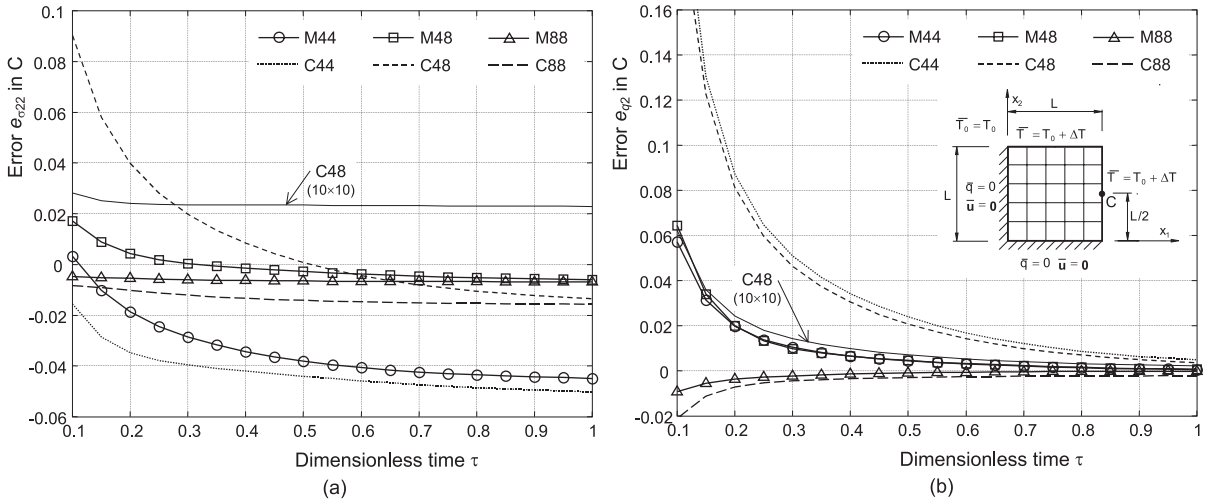

Fig. 7. Test 2 – error time histories in C: (a) normal stress σ_{22} and (b) heat flux q_2.

Table 3
Test 2 – errors in displacement u_1 in A, in temperature in B, and in normal stress σ_{22} and heat flux q_2 in C (see Figs. 6 and 7)

Element	Errors	$\tau = 0.1$	$\tau = 0.3$	$\tau = 0.5$	$\tau = 0.7$	$\tau = 0.9$
M44	$e_{u1} \times 10^{-3}$	0.2919	1.1710	1.7281	1.8343	1.9043
	$e_T \times 10^{-3}$	−9.3088	−2.3783	−0.4079	0.0386	0.1054
	$e_{\sigma 22} \times 10^{-2}$	0.3462	−2.8204	−3.8948	−4.2729	−4.4914
	$e_{q2} \times 10^{-2}$	5.7521	1.0599	0.4671	0.2221	0.1048
M48	$e_{u1} \times 10^{-3}$	1.8754	0.3040	0.0209	−0.1589	−0.2688
	$e_T \times 10^{-3}$	−10.0928	−2.8230	−0.4833	0.1000	0.1551
	$e_{\sigma 22} \times 10^{-2}$	1.7141	0.0409	−0.2751	−0.4590	−0.5664
	$e_{q2} \times 10^{-2}$	6.4608	1.0094	0.4775	0.2482	0.1252
M88	$e_{u1} \times 10^{-3}$	−0.1379	−0.3468	−0.3785	−0.3889	−0.3923
	$e_T \times 10^{-3}$	−0.3371	−0.4943	−0.2496	−0.1189	−0.0559
	$e_{\sigma 22} \times 10^{-2}$	−0.4853	−0.5995	−0.6513	−0.6717	−0.6794
	$e_{q2} \times 10^{-2}$	−0.9290	−0.2240	−0.0954	−0.0420	−0.0185
C44	$e_{u1} \times 10^{-3}$	12.4916	5.7186	3.5191	2.8145	2.2084
	$e_T \times 10^{-3}$	7.2313	20.2367	11.2207	5.7158	2.8251
	$e_{\sigma 22} \times 10^{-2}$	−1.5645	−3.9592	−4.4048	−4.7363	−4.9492
	$e_{q2} \times 10^{-2}$	22.5337	4.9547	2.2500	1.0611	0.4960
C48	$e_{u1} \times 10^{-3}$	11.2958	4.1125	2.0889	1.2416	0.8897
	$e_T \times 10^{-3}$	7.1854	16.8633	8.9090	4.3852	2.1143
	$e_{\sigma 22} \times 10^{-2}$	9.0387	1.9854	0.0766	−0.8066	−1.2252
	$e_{q2} \times 10^{-2}$	21.4100	4.5550	1.9954	0.9138	0.4170
C88	$e_{u1} \times 10^{-3}$	1.0717	0.5791	0.4224	0.3514	0.3189
	$e_T \times 10^{-3}$	3.3567	2.1342	0.9853	0.4470	0.2020
	$e_{\sigma 22} \times 10^{-2}$	−0.8335	−1.2075	−1.4187	−1.5139	−1.5565
	$e_{q2} \times 10^{-2}$	−2.0821	−0.3411	−0.1872	−0.1037	−0.0530

Table 4
Test 2 – number of degrees of freedom of the semidiscrete system of equations

Number of degrees of freedom	M44 5×5	M48 5×5	M88 5×5	C44 5×5	C48 5×5	C88 5×5	C48 10×10
Displacement	72	192	192	72	192	192	682
Temperature	100	100	200	36	36	96	121
Total	172	292	392	108	228	288	803

flux in spite of its smaller number of temperature degrees of freedom. Finally, as noticed in the previous test, the error curves in temperature and heat flux show that element M48 is slightly stiff in predicting the thermal variables.

7. Concluding remarks

The method of analysis herein presented constitutes an alternative approach for linear, coupled thermoelastic analysis from both conceptual and applicative standpoints. The method is of mixed type, and for this feature, it gives direct information on all the quantities involved in the thermoelastic problem. The elastic part is of hybrid type, and the thermal part is based on the mixed flux-temperature formulation. Thermal equilibrium for field heat sources is met a priori. Thermal balance and initial conditions are enforced weakly using temperature as a Lagrange multiplier, and the thermoelastic dissipation term is expressed via the constitutive equations in terms of stress and temperature rates. In the finite element model, temperature within the element is represented independently of temperature on the element boundary. This permits to improve the thermal response without affecting the consistency between stress and temperature approximations.

A comprehensive guideline to a finite element implementation is presented. Three quadrilateral elements are proposed and their qualities are shown through some test cases, drawing a comparison with the standard approach based on displacement and temperature interpolations. In all the tests performed, the mixed elements exhibit a good accuracy over all the time interval of interest, even though relatively coarse meshes are used. Moreover, the mixed elements perform considerably better than the compatible ones with equal number of nodes, especially in the short term response. Comparable overall accuracy can be obtained with compatible finite elements by properly refining the semidiscretization, but a larger number of degrees of freedom is required on the whole. Finally, the mixed model shows a reduced sensitivity to element geometry distortions. In the authors' experience, the better overall accuracy of the mixed model presented generally offsets the computation burden which is higher than the one required by the standard finite element approach based on displacements and temperature. Therefore, the mixed model appears to be reliable and effective for coupled thermoelastic analysis.

Acknowledgements

The authors acknowledge the partial support by the Ministry for University and Scientific and Technological Research (MURST), and partial support by the Italian National Research Council (CNR, contribution No. 97.03129.CT07). Numerical developments were performed at Laboratorio di Meccanica Computazionale (LAMC), DISTART, Università di Bologna, Bologna, Italy.

Appendix A

Explicit form of statement (22):

$$\begin{aligned}
&\int_I \sum_e \Bigg\{ \int_{B_e} \delta\boldsymbol{\sigma} \cdot \big[-\mathbf{C}^{-1}\boldsymbol{\sigma} + \operatorname{symgrad}\mathbf{u} - \mathbf{A}(T-T_0)\big]\,\mathrm{d}V - \int_{\partial B_{ue}} \delta\boldsymbol{\sigma}\mathbf{n}\cdot(\mathbf{u}-\bar{\mathbf{u}})\,\mathrm{d}S \\
&\quad + \int_{B_e} \delta\mathbf{u}\cdot(\operatorname{div}\boldsymbol{\sigma}+\mathbf{p})\mathrm{d}V + \int_{\partial B_{te}} \delta\mathbf{u}\cdot(\boldsymbol{\sigma}\mathbf{n}-\bar{\mathbf{t}})\,\mathrm{d}S \\
&\quad - \int_{B_e} \delta\mathbf{q}\cdot\big(\mathbf{k}^{-1}\mathbf{q}+\operatorname{grad}T\big)\mathrm{d}V + \int_{\partial B_{Te}} \delta\tilde{q}(\tilde{T}-\bar{T})\,\mathrm{d}S + \int_{\partial B_{Te}} \delta\tilde{T}(\tilde{q}-\mathbf{q}\cdot\mathbf{n})\,\mathrm{d}S \\
&\quad + \int_{B_e} \delta T\Big(\operatorname{div}\mathbf{q} - \gamma + T_0\mathbf{C}\mathbf{A}\cdot(\operatorname{symgrad}\mathbf{u})^{\cdot} + \rho c\dot{T}\Big)\mathrm{d}V - \int_{\partial B_{qe}} \delta\tilde{T}(\mathbf{q}\cdot\mathbf{n}-\bar{q})\,\mathrm{d}S \\
&\quad - \int_{\partial B_{ce}} \delta\tilde{T}\Big[\mathbf{q}\cdot\mathbf{n} - \kappa(\tilde{T}-T_c)\Big]\mathrm{d}S + \int_{\partial B_e} \delta\mathbf{q}\cdot\mathbf{n}(T-\tilde{T})\,\mathrm{d}S\Bigg\}\mathrm{d}t \\
&\quad + \int_I \sum_j \Bigg\{ \int_{\rho_j} \delta T\Big[(\mathbf{q}\cdot\mathbf{n})_j^+ + (\mathbf{q}\cdot\mathbf{n})_j^-\Big] + \int_{\rho_j} \delta\mathbf{u}\cdot\Big[(\boldsymbol{\sigma}\mathbf{n})_j^+ + (\boldsymbol{\sigma}\mathbf{n})_j^-\Big]\Bigg\}\mathrm{d}t \\
&\quad - \sum_e \int_{B_e} \delta T|_0 \rho c(T|_0 - \bar{T}_0)\,\mathrm{d}V = 0 \quad \forall(\delta\mathbf{u},\delta\boldsymbol{\sigma},\delta T,\delta\mathbf{q},\delta\tilde{T},\delta\tilde{q}).
\end{aligned}$$

Appendix B

(I) The expressions of matrices and vectors in Eq. (47) are

$$\begin{aligned}
&\hat{\mathbf{W}} = \int_{B_e} \chi\rho c\,\mathbf{N}_T^{\mathrm{T}}\mathbf{N}_T\,\mathrm{d}V,\ \ \boldsymbol{\Lambda} = \int_{B_e} \mathbf{P}_h^{\mathrm{T}}\mathbf{A}\mathbf{N}_T\,\mathrm{d}V,\ \ \mathbf{W} = \int_{B_e} \rho c\,\mathbf{N}_T^{\mathrm{T}}\mathbf{N}_T\,\mathrm{d}V, \\
&\mathbf{H}_\beta = \int_{B_e} \mathbf{P}_h^{\mathrm{T}}\mathbf{C}^{-1}\mathbf{P}_h\,\mathrm{d}V,\ \ \mathbf{H}_\psi = \int_{B_e} \mathbf{L}_\psi^{\mathrm{T}}\mathbf{k}^{-1}\mathbf{L}_\psi\,\mathrm{d}V,\ \ \mathbf{g}_\psi = \int_{B_e} \mathbf{L}_\psi^{\mathrm{T}}\mathbf{k}^{-1}\mathbf{q}_\gamma\,\mathrm{d}V, \\
&\mathbf{G}_{\tilde{\tau}} = \int_{\partial B_e} \mathbf{N}_{\tilde{T}}^{\mathrm{T}}\mathbf{n}^{\mathrm{T}}\mathbf{L}_\psi\,\mathrm{d}S,\ \ \mathbf{G}_\tau = \Big|\mathbf{0}\ \int_{B_e} \mathbf{N}_T^{\mathrm{T}}\operatorname{div}\mathbf{L}_t\,\mathrm{d}V\Big|,\ \ \mathbf{g}_{\tilde{\tau}} = \int_{\partial B_e} \mathbf{N}_{\tilde{T}}^{\mathrm{T}}\mathbf{n}^{\mathrm{T}}\mathbf{q}_\gamma\,\mathrm{d}S, \\
&\mathbf{G}_v = \int_{\partial B_e} \mathbf{N}_u^{\mathrm{T}}\mathbf{N}^{\mathrm{T}}\mathbf{P}_h\,\mathrm{d}S,\ \ \mathbf{g}_\beta = \int_{B_e} \mathbf{P}_h^{\mathrm{T}}(\mathbf{C}^{-1}\boldsymbol{\sigma}_p - T_0\mathbf{A})\,\mathrm{d}V,\ \ \mathbf{g}_v = \int_{\partial B_e} \mathbf{N}_u^{\mathrm{T}}\mathbf{N}^{\mathrm{T}}\boldsymbol{\sigma}_p\,\mathrm{d}S, \\
&\boldsymbol{\tau}_0 = \int_{B_e} \rho c\,\mathbf{N}_T^{\mathrm{T}}\bar{T}_0\,\mathrm{d}V,\ \ \mathbf{h}_v = \int_{\partial B_e} \mathbf{N}_u^{\mathrm{T}}\mathbf{t}\,\mathrm{d}S,\ \ \mathbf{h}_{\tilde{\tau}} = \int_{\partial B_e} \mathbf{N}_{\tilde{T}}^{\mathrm{T}} q\,\mathrm{d}S,
\end{aligned}$$

where $\boldsymbol{\psi}_{ht}^{\mathrm{T}} = |\,\boldsymbol{\psi}_h^{\mathrm{T}} \quad \boldsymbol{\psi}_t^{\mathrm{T}}\,|$, $\mathbf{L}_\psi = |\,\mathbf{L}_h \quad \mathbf{L}_t\,|$, and $\mathbf{N}$ is the matrix containing the direction cosines of the outward normal to ∂B_e. If a part of the element boundary lies on ∂B_q, the equivalent thermal load vector is

$$\mathbf{h}_{\tilde{\tau}}^q = \int_{\partial B_e \cap \partial B_q} \mathbf{N}_{\tilde{T}}^{\mathrm{T}}\bar{q}\,\mathrm{d}S.$$

Moreover, if a part of the element boundary lies on ∂B_c, the term due to convective heat exchange in Eq. (43) reads as

$$\int_{\partial B_e \cap \partial B_c} \tfrac{1}{2}\kappa\Big(\mathbf{N}_{\tilde{T}}\tilde{\boldsymbol{\tau}} - T_c\Big)^2\mathrm{d}S,$$

and the resulting thermal load vector is obtained by differentiating the above term with respect to $\tilde{\boldsymbol{\tau}}$:

$$\mathbf{h}^c_{\tilde{\tau}} = \mathbf{K}_c \tilde{\boldsymbol{\tau}}_{\partial B_c} - \bar{\mathbf{h}}_c,$$

where vector $\tilde{\boldsymbol{\tau}}_{\partial B_c}$ collects the components of $\tilde{\boldsymbol{\tau}}$ relative to ∂B_c and

$$\mathbf{K}_c = \frac{1}{2}\int_{\partial B_e \cap \partial B_c} \kappa \mathbf{N}^{\mathrm{T}}_{\tilde{T}} \mathbf{N}_{\tilde{T}}\, \mathrm{d}S, \qquad \bar{\mathbf{h}}_c = \frac{1}{2}\int_{\partial B_e \cap \partial B_c} \kappa \mathbf{N}_{\tilde{T}} T_c\, \mathrm{d}S.$$

(II) The expressions of matrices and vectors in Eq. (48) are

$$\mathbf{K}_v = \mathbf{G}_v \mathbf{H}_\beta^{-1} \mathbf{G}_v^{\mathrm{T}}, \quad \mathbf{K}_{v\tau} = \mathbf{G}_v \mathbf{H}_\beta^{-1} \boldsymbol{\Lambda}, \quad \mathbf{p}_v = \mathbf{g}_v - \mathbf{G}_v \mathbf{H}_\beta^{-1} \mathbf{g}_\beta,$$

$$\mathbf{K}_{\tilde{\tau}} = \mathbf{G}_{\tilde{\tau}} \mathbf{H}_\psi^{-1} \mathbf{G}_{\tilde{\tau}}^{\mathrm{T}}, \quad \mathbf{K}_{\tilde{\tau}\tau} = \mathbf{G}_{\tilde{\tau}} \mathbf{H}_\psi^{-1} \mathbf{G}_\tau^{\mathrm{T}}, \quad \mathbf{K}_\tau = \mathbf{G}_\tau \mathbf{H}_\psi^{-1} \mathbf{G}_\tau^{\mathrm{T}}$$

$$\mathbf{p}_{\tilde{\tau}} = \mathbf{g}_{\tilde{\tau}} + \mathbf{G}_{\tilde{\tau}} \mathbf{H}_\psi^{-1} \mathbf{g}_\psi, \quad \mathbf{p}_\tau = -\mathbf{G}_\tau \mathbf{H}_\psi^{-1} \mathbf{g}_\psi, \quad \mathbf{M}_\tau = \hat{\mathbf{W}} - T_0 \boldsymbol{\Lambda}^{\mathrm{T}} \mathbf{H}_\beta^{-1} \boldsymbol{\Lambda}.$$

Appendix C

Element stress and flux representations

Element M44

$$\mathbf{P}_h = \begin{vmatrix} 1 & 0 & 0 & \bar{x}_2 & 0 & \bar{x}_1 & 0 \\ 0 & 1 & 0 & 0 & \bar{x}_1 & 0 & \bar{x}_2 \\ 0 & 0 & 1 & 0 & 0 & -\bar{x}_2 & -\bar{x}_1 \end{vmatrix},$$

$$\mathbf{L}_h = \begin{vmatrix} 1 & 0 & 0 & \bar{x}_2 & \bar{x}_1 \\ 0 & 1 & \bar{x}_1 & 0 & -\bar{x}_2 \end{vmatrix},$$

$$\mathbf{L}_t = \begin{vmatrix} \bar{x}_1 & \bar{x}_1^2 & 0 & 2\bar{x}_1\bar{x}_2 & \bar{x}_2^2 & 3\bar{x}_1^2\bar{x}_2 & \bar{x}_2^3 \\ \bar{x}_2 & 0 & \bar{x}_2^2 & \bar{x}_1^2 & 2\bar{x}_1\bar{x}_2 & \bar{x}_1^3 & 3\bar{x}_1\bar{x}_2^2 \end{vmatrix}.$$

Element M48

$$\mathbf{P}_h = \begin{vmatrix} 1 & 0 & 0 & \bar{x}_2 & 0 & \bar{x}_1 & 0 & \bar{x}_1^2 & 2\bar{x}_1\bar{x}_2 & \bar{x}_2^2 & 0 & 0 & 0 & 0 & \bar{x}_1^3 & 3\bar{x}_1^2\bar{x}_2 & 3\bar{x}_1\bar{x}_2^2 & \bar{x}_2^3 \\ 0 & 1 & 0 & 0 & \bar{x}_1 & 0 & \bar{x}_2 & \bar{x}_2^2 & 0 & 0 & \bar{x}_1^2 & 2\bar{x}_1\bar{x}_2 & \bar{x}_1^3 & 3\bar{x}_1^2\bar{x}_2 & 3\bar{x}_1\bar{x}_2^2 & \bar{x}_2^3 & 0 & 0 \\ 0 & 0 & 1 & 0 & 0 & -\bar{x}_2 & -\bar{x}_1 & -2\bar{x}_1\bar{x}_2 & -\bar{x}_2^2 & 0 & 0 & -\bar{x}_1^2 & 0 & -\bar{x}_1^3 & -3\bar{x}_1^2\bar{x}_2 & -3\bar{x}_1\bar{x}_2^2 & -\bar{x}_2^3 & 0 \end{vmatrix},$$

$$\mathbf{L}_h = \begin{vmatrix} 1 & 0 & 0 & \bar{x}_2 & \bar{x}_1 \\ 0 & 1 & \bar{x}_1 & 0 & -\bar{x}_2 \end{vmatrix},$$

$$\mathbf{L}_t = \begin{vmatrix} \bar{x}_1 & \bar{x}_1^2 & 0 & 2\bar{x}_1\bar{x}_2 & \bar{x}_2^2 & 3\bar{x}_1^2\bar{x}_2 & \bar{x}_2^3 & \bar{x}_1^3 & 0 & \bar{x}_1\bar{x}_2^2 & \bar{x}_1^4 & 4\bar{x}_1^3\bar{x}_2 & 3\bar{x}_1^2\bar{x}_2^2 & 2\bar{x}_1\bar{x}_2^3 & \bar{x}_2^4 & 0 \\ \bar{x}_2 & 0 & \bar{x}_2^2 & \bar{x}_1^2 & 2\bar{x}_1\bar{x}_2 & \bar{x}_1^3 & 3\bar{x}_1\bar{x}_2^2 & 0 & \bar{x}_2^3 & \bar{x}_1^2\bar{x}_2 & 0 & \bar{x}_1^4 & 2\bar{x}_1^3\bar{x}_2 & 3\bar{x}_1^2\bar{x}_2^2 & 4\bar{x}_1\bar{x}_2^3 & \bar{x}_2^4 \end{vmatrix}.$$

Element M88

$$\mathbf{P}_h = \begin{vmatrix} 1 & 0 & 0 & \bar{x}_2 & 0 & \bar{x}_1 & 0 & \bar{x}_1^2 & 2\bar{x}_1\bar{x}_2 & \bar{x}_2^2 & 0 & 0 & 0 & 0 & \bar{x}_1^3 & 3\bar{x}_1^2\bar{x}_2 & 3\bar{x}_1\bar{x}_2^2 & \bar{x}_2^3 \\ 0 & 1 & 0 & 0 & \bar{x}_1 & 0 & \bar{x}_2 & \bar{x}_2^2 & 0 & 0 & \bar{x}_1^2 & 2\bar{x}_1\bar{x}_2 & \bar{x}_1^3 & 3\bar{x}_1^2\bar{x}_2 & 3\bar{x}_1\bar{x}_2^2 & \bar{x}_2^3 & 0 & 0 \\ 0 & 0 & 1 & 0 & 0 & -\bar{x}_2 & -\bar{x}_1 & -2\bar{x}_1\bar{x}_2 & -\bar{x}_2^2 & 0 & 0 & -\bar{x}_1^2 & 0 & -\bar{x}_1^3 & -3\bar{x}_1^2\bar{x}_2 & -3\bar{x}_1\bar{x}_2^2 & -\bar{x}_2^3 & 0 \end{vmatrix},$$

$$\mathbf{L}_h = \begin{vmatrix} 1 & 0 & 0 & \bar{x}_2 & \bar{x}_1 \\ 0 & 1 & \bar{x}_1 & 0 & -\bar{x}_2 \end{vmatrix},$$

$$\mathbf{L}_t = \begin{vmatrix} \bar{x}_1 & \bar{x}_1^2 & 0 & 2\bar{x}_1\bar{x}_2 & \bar{x}_2^2 & 3\bar{x}_1^2\bar{x}_2 & \bar{x}_2^3 & \bar{x}_1^3 & 0 & \bar{x}_1\bar{x}_2^2 & \bar{x}_1^4 & 4\bar{x}_1^3\bar{x}_2 & 3\bar{x}_1^2\bar{x}_2^2 & 2\bar{x}_1\bar{x}_2^3 & \bar{x}_2^4 & 0 \\ \bar{x}_2 & 0 & \bar{x}_2^2 & \bar{x}_1^2 & 2\bar{x}_1\bar{x}_2 & \bar{x}_1^3 & 3\bar{x}_1\bar{x}_2^2 & 0 & \bar{x}_2^3 & \bar{x}_1^2\bar{x}_2 & 0 & \bar{x}_1^4 & 2\bar{x}_1^3\bar{x}_2 & 3\bar{x}_1^2\bar{x}_2^2 & 4\bar{x}_1\bar{x}_2^3 & \bar{x}_2^4 \end{vmatrix}.$$

References

Atarashi, T., Minagawa, S., 1992. Transient coupled-thermoelastic problem of heat conduction in a multilayered composite plate. Int. J. Engng. Sci. 30, 1543–1550.

Askar Altay, G., Cengiz Dökmeci, M., 1996. Some variational principles for linear coupled thermoelasticity. Int. J. Solids Struct. 33, 3937–3948.

Atluri, S.N., Gallagher, G.H., Zienkiewicz, O.C., 1983. Hybrid and Mixed Finite Element Methods. Wiley, Chichester.

Ben-Amoz, M., 1965. On a variational theorem in coupled thermoelasticity. J. Appl. Mech. 32, 943–945.

Biot, M.A., 1956. Thermoelasticity and irreversible thermodynamics. J. Appl. Phys. 27, 250–253.

Boley, B.A., Weiner, J., 1960. Theory of Thermal Stresses. Wiley, London.

Brezzi, F., Fortin, M., 1991. Mixed and Hybrid Finite Element Methods. Springer, New York.

Cannarozzi, A.A., Momanyi, F.X., Ubertini, F., 2000. A hybrid flux model for heat conduction problems. Int. J. Numer. Meth. Engng. 47, 1731–1749.

Cannarozzi, A.A., Mondelli, M., 1998. In tema di irregolarità di geometria negli elementi finiti parametrici. In: Proceedings of XI Convegno Italiano di Meccanica Computazionale-GIMC, Trento, Italy.

Cannarozzi, A.A., Ubertini, F., 1998. Un modello misto in analisi termoelastica. In: Proc. of XI Convegno Italiano di Meccanica Computazionale - GIMC, Trento, Italy.

Cannarozzi, A.A., Momanyi, F.X., Ubertini, F., 1999. A hybrid flux axisymmetric model for thermal analysis. DISTART, Internal Report 22, University of Bologna, Italy, Comp. Struct., submitted for publication.

Carlson, D.E., 1972. Linear Thermoelasticity. In: Truesdell, C. (Ed.), Handbuch der Physik, vol. 6a/2. Springer, Berlin, pp. 297–346.

Carter, J.P., Booker, J.R., 1989. Finite element analysis of coupled thermoelasticity. Comp. Struct. 31, 73–80.

Danilovskaya, V.I., 1950. Thermal stresses in an elastic half-space arising after a sudden heating of its boundary. Prikl. Mat. Mekh. 14, 316–318.

de Miranda, S., Ubertini, F., 1999. On the consistency of finite element models in thermoelastic analysis. DISTART, Internal Report 21, University of Bologna, Italy, Comp. Meth. Appl. Mech. Engng., in press.

Fraeijs de Veubeke, B.M., Hogge, M.A., 1972. Dual analysis for heat conduction problems by finite elements. Int. J. Num. Meth. Engng. 5, 65–82.

Herrmann, G., 1963. On variational principles in thermoelasticity and heat conduction. Q. Appl. Maths. 22, 151–155.

Hogge, M.A., Fraeijs de Veubeke, B.M., 1972. Heat conduction. CISM-Centro Internazionale di Scienze Meccaniche, Udine.

Hughes, T.J.R., 1987. The finite element method. In: Linear Static and Dynamic Finite Element Analysis. Prentice-Hall, Englewood Cliffs, NJ.

Iesan, D., 1966. Principes variationnels dans la théorie de la thermoélasticité couplee, Analele Stiint. Univ. ''A.I. Cuza'' Iasi, Sect. I. Matematica 12, 439–456.

Keramidas, G.A., Ting, E.C., 1976. A finite element formulation for thermal stress analysis. I. Variational formulation. II. Finite element formulation. Nucl. Engng. Des. 39, 267–287.

Mancuso, M., Ubertini, F., Momanyi, F.X., 1998. Time Continuous Galerkin methods for linear heat conduction. DISTART, Internal Report 16, University of Bologna, Italy, Comp. Meth. Appl. Mech. Engng., in press.

Nickell, R.E., Sackman, J.L., 1968. Approximate solution in linear coupled thermoelasticity. ASME J. Appl. Mech. 35, 255–266.

Nowacki, W., 1986. Thermoelasticity. Pergamon Press, New York.

Pian, T.H.H., 1973. Hybrid Models. In: Fenves, S.J., Perrone, N., Robinson, R., Schonbrick, W.C. (Eds.), Numerical and Computer Methods in Structural Mechanics. Academic Press, New York, pp. 50–80.

Prathap, G., Naganarayana, B.P., 1995. Consistent thermal stress evaluation in finite elements. Comp. Struct. 54, 415–426.

Prigogine, I., 1961. Thermodynamics of Irreversible Processes. Wiley, New York.

Rafalski, P., 1968. A variational principle for the coupled thermoelastic problem. Int. J. Engng. Sci. 6, 465–471.

Rao, D.M., Sinha, P.K., 1997. Finite element coupled thermostructural analysis of composite beams. Comp. Struct. 63, 539–549.

Sze, K.Y., Chow, C.L., Wanji, C., 1992. On invariance of isoparametric hybrid/mixed elements. Comm. Appl. Numer. Meth. 8, 385–406.

Tay, T.E., 1992. Finite element analysis of thermoelastic coupling in composites. Comp. Struct. 43, 107–112.

Tamma, K.K., Namburu, R.R., 1991. Unified finite element transient analysis formulations for interdisciplinary thermal structural problems. In: Lewis, R.W., Chin, J.H., Homsy, G.M. (Eds.), Numerical Methods. In: Thermal Problems, vol. 7. Part 2, Pineridge Press, Swansea, UK. pp. 1238–1251.

Ubertini, F., 1998. Formulazioni Variazionali e Sviluppi Computazionali in Termoelasticità. Ph.D. Dissertation, University of Bologna, Italy.

Washizu, K., 1982. Variational Methods in Elasticity and Plasticity. Pergamon Press, Oxford.

Wood, W.L., 1990. Practical Time-stepping Schemes. Clarendon Press, Oxford.

Xue, W.-M., Atluri, S.N., 1985. Existence and stability, and discrete BB and rank conditions for general mixed-hybrid finite elements in elasticity. In: Spilker, R.L., Reed, K.W. (Eds.), Hybrid and Mixed Finite Element Methods. ASME, New York AMD vol. 73, pp. 91–112.

Zanaboni, O., 1936. Il problema della funzione delle tensioni in un sistema spaziale isotropo. Bollettino U.M.I., XV, 2, 71–76.

Zhu, Y.Y., Cescotto, S., 1995. Unified and mixed formulation of the 4-node quadrilateral elements by assumed strain method: application to thermomechanical problems. Int. J. Num. Meth. Engng. 38, 685–716.

Zienkiewicz, O.C., Taylor, R.L.T., 1989. The Finite Element Method. McGraw-Hill, London.